ULTRASTRUCTURE, HISTOCHEMISTRY, AND MINERALIZATION PATTERNS IN THE ECDYSIAL SUTURE OF THE BLUE CRAB, CALLINECTES SAPIDUS

Carolina Priester

A Thesis Submitted to the
University of North Carolina at Wilmington in Partial Fulfillment
of the Requirements for the Degree of
Master of Science

Department of Biological Sciences

University of North Carolina at Wilmington

2003

Approved by

Advisory Committee

Neil Hadley
Dr. Neil Hadley

Robert Roer
Dr. Robert Roer

Thomas H. Shafer
Dr. Thomas Shafer

Richard M. Dillaman
Dr. Richard Dillaman, Chair

Accepted by

Robert Roer
Dean, Graduate School

This thesis has been prepared in the style and format

consistent with the journal

Journal of Morphology

TABLE OF CONTENTS

ABSTRACT iv

ACKNOWLEDGEMENTS vi

DEDICATION vii

LIST OF TABLES viii

LIST OF FIGURES ix

INTRODUCTION 1

MATERIALS AND METHODS 5

Animals and experimental design 5

Light microscopy 6

Scanning Electron Microscopy 8

RESULTS 11

Histochemistry 11

Lectin affinity 12

Scanning electron microscopy 13

X-ray microanalysis 17

DISCUSSION 21

LITERATURE CITED 56

BIOGRAPHICAL SKETCH 65

ABSTRACT

The ecdysial suture is the region on an arthropod exoskeleton that splits to allow the animal to escape from its old carapace. To understand why this region preferentially splits, I examined the morphology and composition of the intermolt and premolt suture of the blue crab, *Callinectes sapidus,* using light and scanning electron microscopy (SEM). No differences were detected between the suture and the adjacent cuticle with the general dyes acridine orange, hematoxylin and eosin, toluidine blue, periodic acid Schiff or paraldehyde fuchsin. Only three of 22 FITC-labeled lectins differentiated the suture. *Lens culinaris* agglutinin, *Vicia faba* agglutinin, and *Pisum sativum* agglutinin, which have an affinity for fucosylated α-N-acetylglucosamine with mannose dendrimers, bound more intensely to the exocuticle of the suture and less intensely to the endocuticle of the suture. The suture had no setae, and was paralleled by a knobbed ridge. The suture was thinner than the surrounding cuticle, especially in the posterior region where it was also wider. Back-scattered electron (BSE) and secondary electron (SE) observations of the fracture surface of intermolt cuticle showed that in the exocuticle of the suture the prisms were not in-filled with calcium, whereas the prisms of the surrounding cuticle were fully mineralized. BSE analysis of premolt and intermolt, resin-embedded cuticle indicated that the suture was less mineralized than the surrounding cuticle. EDAX non-dispersive X-ray microanalysis further demonstrated that the suture was less calcified than the adjacent calcified cuticle and had significantly lower magnesium and phosphorus concentrations, making the calcite in the suture more soluble. While the suture is very similar to non-suture calcified cuticle in terms of anatomy and histology, it differs in

several aspects: (1) the presence or absence of a type of glycoprotein in the organic matrix, (2) the extent and composition of the mineral deposited and (3) the thickness of the cuticle. These characteristics make the suture mechanically weaker, more soluble and thus more susceptible to the molting fluid produced by the crab. This renders the suture predetermined to fail when stressed by the internal pressure exerted by the swelling of the underlying new exoskeleton, and ensures successful ecdysis.

ACKNOWLEDGEMENTS

I would like to take this opportunity to thank everyone that supported me, in one way or another, and helped me through this Master's program. Many thanks to Dr. Dillaman, who has been an excellent chair and advisor and who got me excited about mineralization in blue crabs. Thanks to my committee members for enriching my work with all the excellent insights and advises. To Mark Gay, thanks a lot for teaching me everything I know about microscopy techniques and image analysis! Thanks to Dr. Scharf for the assistance with the data analysis. To Dr. Shelly Etnier and Dr. Ann Pabst, thank you for the advices and the chats on biomechanics. To my fellow, past and present, graduate students, thanks for the moments of fun, for the support and for helping in keeping the Biology Graduate Student Association alive. It was a great experience!!

I would also like to acknowledge and thank my mother, my sisters and my uncles for providing love, support and encouragement. Thanks to my friends from Brazil who had to deal with me not answering emails and hardly ever calling but who had words of encouragement at any opportunity they had of contacting me. Special thanks to Luis for believing in me and encouraging me. And thanks to Kobe and Malone for cheering me up.

Funding for this project was provided by Sigma Xi Grant-in-Aid of Research to CP and NSF Grants IBN-0114597 and DBI-9978614 to RMD. This project was also supported by instrumentation grants to RMD: ONR 99-1-0690, NSF DBI-9970099, NC Biotechnology Center 9903-IDG-1014.

DEDICATION

I dedicate this thesis to my grandmother, Marion S. Staub, who has not lived to see my accomplishments; to my mother, Elizabeth M.S. Priester, for the support; and to Luis E. Baptista, for believing in me and encouraging me throughout my studies and work – you are the most wonderful person I've ever met.

LIST OF TABLES

Table Page

1. Concentration (Wt%) of elements in suture and adjacent cuticle regions for molt stages $C_4 - D_3$ 53

2. Statistical analysis of elemental concentrations among regions of the cuticle 54

3. Mean values for the ratios of Ca/Mg (a) and Ca/P (b) at the different cuticle regions 55

LIST OF FIGURES

Figure Page

1. Light micrographs of intermolt (C_4) cuticle containing the suture (arrowhead) stained 34

2. Fluorescence images of intermolt cuticle regions containing the suture, fixed in alcoholic formalin 36

3. a & b. Fluorescence images of cuticle regions containing the suture, fixed in (a) alcoholic formalin or (b) Bouin's 38

4. SEM micrographs of the region of the suture (arrows) of an intermolt cuticle showing external (a, c, and d) and internal (b) surfaces 40

5. SEM micrographs of fractured samples of intermolt crabs from posterior (a-e) and anterior (f) sectors of the carapace 42

6. BSE micrographs of embedded and cut samples containing the suture of crabs in intermolt and D_1'' stages 44

7. BSE micrographs of embedded and cut samples containing the suture of crabs in early and late D_2 stages 46

8. Mean cuticle thickness (μm) (± SEM) versus (a) region of the cuticle; (b) carapace location; and (c) stage of the molt cycle 48

9. X-ray maps of an embedded anterior piece of cuticle from an intermolt crab containing the suture 50

10. Plots of calcium concentrations (Wt %) among cuticle regions against magnesium (a) and phosphorous (b) concentrations (Wt %) 52

INTRODUCTION

The cuticle of the blue crab is divided into four layers. Epicuticle, the outermost layer, represents about 2% of the total cuticle thickness (Hegdahl et al., 1977c). Below the epicuticle are the exocuticle, endocuticle and the membranous layer, respectively (Green and Neff, 1972; Travis and Friberg, 1963; Roer and Dillaman, 1993). The exocuticle is approximately 24% of the total cuticle thickness and is calcified (Hegdahl et al., 1977b and 1977c). It has a tanned, chitin-protein matrix arranged in lamellae (Green and Neff, 1972). Both epi- and exocuticle are deposited during premolt, and are calcified postecdysis (Hegdahl et al., 1977b and 1977c). Endocuticle, which constitutes approximately 74% of total cuticle thickness, is not tanned, and has a chitin-protein matrix also arranged in lamellae (Dennell, 1947; Travis, 1955a; Hegdahl et al., 1977a; Giraud-Guille, 1984b). This layer is calcified as it is being deposited and becomes as heavily calcified as the epicuticle and exocuticle (Green and Neff, 1972; Hegdahl et al., 1977a and 1977b). The mineral in these three layers is calcium carbonate ($CaCO_3$) in the form of calcite (Travis, 1963; Simkiss, 1975). The membranous layer is the innermost layer, and it also has a chitin-protein matrix. However, it is neither calcified nor tanned (Green and Neff, 1972). The cuticular layers contain chitin and protein, and have been demonstrated by Marlowe et al. (1994) to also contain additional glycoproteins and carbohydrate residues.

Underneath the four layers of cuticle is the hypodermis (epithelial tissue) (Travis, 1955a and 1955b; Travis, 1957; Travis, 1965; and Roer and Dillaman, 1984) that is responsible for secreting the new cuticle as well as the molting fluid (Travis, 1955a and

1955b; Travis, 1957; Travis, 1965; Neville, 1975; Skinner, 1985; O'Brien and Skinner, 1987; O'Brien and Skinner, 1988; Spindler-Barth et al., 1990). As the cuticle is deposited, the hypodermis leaves behind in the cuticle numerous, small, branching cytoplasmic extensions, called pore canals (Green and Neff, 1972; Hegdahl et al., 1977a and 1977b; Compère and Goffinet, 1987a and 1987b). Supposed imprints of the margins of the hypodermal cells are also found in the exocuticle and are thought to be the initial sites of calcification (Travis, 1957; Travis, 1963; Travis, 1965; Hegdahl et al., 1977b; Giraud-Guille, 1984a; Hequembourg, 2002).

In order to grow, crustaceans replace their exoskeleton in a series of events called the molt cycle. The molt cycle has been divided in five stages (A to E) by Drach (1939), with each stage based on cuticle hardness or softness in certain areas (Drach, 1939; Stevenson, 1968; Travis, 1955a). The physiological, biochemical, and histological changes during those stages have been extensively examined (Travis, 1955a and 1955b; Travis, 1957; Johnson, 1980; Roer and Dillaman, 1984; Mangum et al., 1985; Spindler-Barth et al., 1990; Shafer et al., 1995). Also examined has been the pattern of calcification in the new cuticle (Giraud-Guille, 1984a; Skinner, 1962; Travis, 1963; Travis and Friberg, 1963; Travis, 1965; Hequembourg, 2002).

The intermolt or C_4 stage, in which crustaceans spend most of their time, is characterized by the cuticle being completely deposited and fully mineralized (Mangum, 1985; Green and Neff, 1972). Following intermolt is the stage $D_{0,}$ which is activated by crustecdysone, a molting hormone (Freeman, 1980). During this stage the hypodermis separates from the cuticle (apolysis). With the light microscope one detects this stage by the retraction of the setae (Stevenson, 1972; Reaka, 1975; Elliott and Dillaman, 1999).

Separation is caused by secretion, from the hypodermis into the ecdysial space, of a molting fluid containing digestive, chitinolytic enzymes including chitinase, chitobiase and N-acetyl-β-D-glucosaminidase (Green and Neff, 1972; Neville, 1975; O'Brien and Skinner, 1987, 1988; Spindler and Buchholz, 1988; Buchholz, 1989; Spindler and Funke, 1989; Spindler-Barth et al., 1990; Compère et al., 1998). These enzymes promote the dissolution of the membranous layer of the old cuticle (Skinner, 1962; Skinner, 1985) and subsequently the partial degradation of the calcified layers (Compère et al., 1998). Molting crabs partially resorb the products of the digestion of their old exoskeleton (Spindler and Buchholz, 1988; Compère et al., 1998) and underneath it deposit a new, larger, flexible exoskeleton.

From stage D_1 through D_3, while the new cuticle is being formed, the old cuticle is continuing to be digested (Passano, 1960; Green and Neff, 1972; Stevenson, 1972). By the end of stage D_3 skeletal resorption is at its maximum (Passano, 1960), and the cuticle begins to split at predictable and externally visible sites, the suture (Green and Neff, 1972). Just prior to ecdysis, at stage D_4 (Green and Neff, 1972), the cuticle splits at predictable and externally visible sites in response to expansion of the underlying new cuticle (Passano, 1960; Mangum et al., 1985). These sites appear as lines, called ecdysial lines or clefts, sutures, or lines of weakness or dehiscence (Mangum, 1985; Compère et al., 1998). At stage E the crab emerges from the old exoskeleton and rapidly takes up additional water in order to fully expand its carapace (Passano, 1960; Green and Neff, 1972; Mangum et al., 1985).

Whereas the role of the ecdysial lines in crustaceans has been known and described previously, its ultrastructure and mechanism for splitting have not been investigated in

depth. The edcdysial line of crustaceans has been referred to previously in the literature, but only as an aid in premolt stage classification (Passano, 1960; Green and Neff, 1972; Mangum, 1985; Compère et al., 1998). The only reports of suture morphology and composition are for insects (Chapman, 1982; Kathirithamby et al., 1990; Hadley, 1994). However, since the cuticle of crustaceans is composed of the same number of layers as the cuticle of insects (Neville, 1975; Hadley, 1994), comparisons between insects and crustaceans can be useful. In the small number of insects where it has been examined, the cuticle at the suture has been shown to be different from the adjacent cuticle. For example, Chapman (1982) demonstrated that in larval hemimetabolous insects the exocuticle is absent at the suture line; only endocuticle and epicuticle are present. Supposedly endocuticle is preferentially digested by molting fluid and a line of weakness is formed. However, Kathirithamby et al. (1990) report that in the puparium cap of *Elenchus tenuicornis* (Insecta: Strepsiptera) all the layers, including exocuticle, are present at the suture. In this case the exocuticle is untanned, thereby rendering it different from the adjacent exocuticle and more easily digested by molting fluid. This would leave the carapace attached only at the epicuticle, thereby forming a line of weakness (Kathirithamby et al., 1990).

Crustacean cuticle differs from insect cuticle in several aspects. For example, crustaceans mineralize many portions of their cuticle (Drach, 1939; Passano, 1960; Green and Neff, 1972; Giraud-Guille, 1984a; Roer and Dillaman, 1984; Hequembourg, 2002) whereas insect cuticle is, generally, not calcified. One exception to this is the fly larva *Exeretonevra angustifrons*, whose cuticle has been found to contain amorphous calcium phosphate (Rasch et al., 2003). However, like the ultrastructure of the suture line in

crustaceans, the calcium content of the suture has never been measured. A difference in ultrastructure and/or calcium content between the suture line and the adjacent cuticle might explain why this region is preferentially digested by the molting fluids. Conversely, it could simply indicate that this region is mechanically weaker, thus splitting when internal pressure increases due to water uptake prior to ecdysis.

The objective of this investigation is to describe the functional morphology and mineral distribution of the suture line in the blue crab, *Callinectes sapidus*, using scanning electron microscopy and light microscopic histochemistry. Four hypotheses will be tested concerning the structure, composition, mineral content, and dimensions of the suture. The first hypothesis is that the ventral suture line morphology does not vary from that of the cuticle surrounding it. The second hypothesis is that the organic matrix of the suture line of crustaceans has the same morphology and composition as the adjacent cuticle. The third hypothesis is that the mineral content of the suture does not vary from that of the surrounding cuticle. The fourth and final hypothesis is that the suture dimensions do not vary across regions, these regions being the anterior, middle, and posterior portions of the carapace.

MATERIALS AND METHODS

Animals and experimental design

Blue crabs were obtained from Endurance Sea Food, Kill Devil Hills, NC, or Scott Rader, Wilmington, NC. Females were used because shape of the apron allows differentiation between mature and immature individuals. Immature crabs were expected to molt periodically until they reach maturity, whereas mature individuals probably

would not. Consequently, in this study only immature individuals ranging in length from 5 cm to 11.8 cm were used.

Crabs were collected at intermolt, stage C_4, and premolt, stages D_0 through D_4 (Drach, 1939). From each individual an area was cut from the ventral side including the ecdysial suture and approximately 5mm of adjacent cuticle on each side of the suture. Several different pieces were collected along the suture from the posterior to the anterior end of the carapace.

Light microscopy

Cuticle samples were collected and fixed in Bouin's fixative (Presnell and Schreibman, 1997), or in alcoholic formalin (9:1) (Marlowe et al., 1994). Pieces were fixed for 5 days, with a change of the fixatives after the first 24 hours. Pieces fixed in alcoholic formalin were decalcified in 10% EDTA in 0.1M Tris buffer, pH 7.6, for 2 weeks or until they were flexible. Samples were then rinsed in 0.1M Tris buffer, pH 7.6, and dehydrated through an ascending series of ethanol (50, 70, 95, 100%) for 30 minutes, twice each. Tissue samples were then cleared in toluene and embedded in paraffin. Sections 8μm thick were attached to slides with Mayer's egg white albumin (Presnell and Schreibman, 1997), except for sections to be stained with acridine orange and lectins. Sections were deparaffinized, rehydrated through a descending series of acetones (100, 90, 70, 50% acetone) to deionized water or crab physiological saline (Roer, 1980). Lectin and acridine orange staining followed the techniques described by Marlowe et al. (1994) and Marlowe and Dillaman (1995), respectively. For histological staining, the

slides were dehydrated through a series of ascending acetones after staining and cover slips were mounted with Permount (Fisher Scientific).

Tissues were stained with periodic acid Schiff stain, hematoxylin and eosin, 0.1% toluidine blue in 0.2M sodium borate buffer, pH 9.2 (Presnell and Schreibman, 1997), paraldehyde fuchsin (Gomori, 1950; Thompson, 1966), or fluorescein isothiocyanate (FITC) labeled lectins. Tissues fixed in alcoholic formalin were also stained with acridine orange (Marlowe and Dillaman, 1995). Preliminary studies were performed using a battery of 21 fluorescent-labeled lectins previously used by Marlowe et al. (1994). When two of these lectins, LCA, *Lens culinaris* agglutinin and PSA, *Pisum sativum* agglutinin (from Vector Laboratories) showed differential binding between the suture line cuticle and the adjacent cuticle, another lectin with similar binding affinity was chosen and used. This third lectin was VFA, *Vicia faba* agglutinin (from EY Laboratories). All three are said to bind to fucosylated α-N-acetylglucosamine with mannose dendrimers (Debray et al., 1981; Young et al., 1996; EY Laboratories). Lectins were used in a concentration of 30 μg/ml in crab physiological saline solution (Roer, 1980). Half a milliliter of the diluted lectin was used to stain each slide. Samples stained with acridine orange or FITC-labeled lectins were observed with an Olympus BH-2 epifluorescence microscope with blue excitation achieved by using a DM500 dichroic mirror with an IF490 excitation filter and a 515-nm barrier filter. Images were collected with a Spot RT digital color camera (Diagnostic Instruments, Inc.).

Scanning Electron Microscopy

Cuticle containing the suture line was obtained by means of cutting along side the suture line with a Dremel cutting and sanding tool. Approximately 5mm were left on each side of the suture line to prevent destruction of the region of interest and to allow surrounding cuticle for comparison to the cuticle of the suture line. From one side of each crab the piece was allowed to air-dry. From the other side of each crab the piece was freeze-dried. The freeze-dried pieces were fractured into smaller pieces. Air-dried samples were mounted on aluminum stubs with colloidal graphite, coated with 6 nm of platinum-palladium (80:20) in a Cressington 208 HR Sputter Coater. Some pieces were mounted for cross-sectional view, others for internal or external view of the suture. Samples were observed with the secondary electron and back-scattered electron modes of the Philips XL30S FEG scanning electron microscope. Another scanning electron microscopy (SEM) mode used was non-dispersive x-ray microanalysis (Phoenix, EDAX Inc.). This mode allowed mapping and quantification of specific elements in the sample. The amounts of each element present were determined by the area under the curve and above background in the energy (keV) vs. intensity (counts) graph for each region analyzed. The software used has a function called Holographic Peak Deconvolution that allowed the peaks to be best fit to each element, separating peaks that were too close to each other.

Surface features were best observed when fractured after freeze-drying or air-drying. In all three detection modes the yield of the electrons or x-rays is affected by geometry between the sample and the detector; however, it is most critical in x-ray mapping, where a smooth surface allows more accurate and reproducible x-ray information about the

specimen. To obtain a smooth surface in each specimen the freeze-dried samples were embedded in Spurr's epoxy resin (Spurr, 1969), then cut and polished. The pieces were attached to aluminum stubs with colloidal graphite so that a cross section of the suture with adjacent cuticle on either side would be visible. Samples were coated with 6nm of platinum-palladium (80:20). Each sample was observed with the scanning electron microscope (SEM), utilizing secondary electron (SE), back-scattered electron (BSE) and Phoenix EDAX non-dispersive x-ray microanalysis modes at 10 kV accelerating voltage. Ten kV was determined to be the best accelerating voltage for these analyses since it is approximately two-fold the energy released by x-rays of the highest atomic number element of interest in the specimen (calcium, with Kα energy of 3.691). The suture line could be seen through the translucent resin block, so two nicks were made on the face of the resin on either side of the suture so that its location in the resin block could be precisely determined when the sample face was viewed in the SEM.

Atomic number differences among regions of the sample were detected with the BSE mode. The calcium content was analyzed using the EDAX ZAF Quantification (Standardless) X-ray microanalysis mode. Areas of approximately 40μm by 40μm were selected and analyzed for element content at the slowest scan rate in different regions of the cuticle, including exocuticle at suture line, exocuticle at adjacent cuticle, upper (outermost) and lower (innermost) endocuticle at suture line, and endocuticle at adjacent cuticle. If the region of the lower endocuticle had been digested away, an area immediately above it was sampled. When the digestion reached the upper endocuticle, no measurements could be taken for the lower endocuticle, consequently reducing the sample size for this region. Spot analysis was not used because it eroded the sample,

altering the geometry between the surface of the sample and x-ray detector thus giving unreliable results. Standardless quantitative data were collected with the relative weight percent and atomic percent of the elements present in the sample recorded. Ratios between collected values were calculated, and since the ratios were greater than one, no transformation for the data was required.

Data were analyzed using single factor analysis of variance - Tukey multiple comparison test with unequal sample sizes (Zar, 1999), the factor being the region of the cuticle. Data were sorted and graphed in Sigma Plot 8.0. For each sample, comprehensive elemental maps of the entire region containing both calcified cuticle and suture were obtained to investigate the spatial distribution of calcium and other selected elements that were found in the square regions of the suture and adjacent cuticle that were analyzed. These elements were carbon, chloride, magnesium, sodium, oxygen, phosphorous, and sulfur. The maps were collected at 512 x 400 resolution, dwell time 100ms, amplifier time 50μs, and 128 frames. Suture and adjacent cuticle thickness were measured from the micrographs of the embedded samples. Thickness of the cuticle was assessed using a 3-way factorial analysis of variance (ANOVA) with cuticle region (suture or adjacent calcified cuticle), carapace measurement location (anterior, middle, or posterior), and stage of the molt cycle (C_4, D_1, or D_2) as main effects. Statistical significance of each of the main effects and interaction terms was evaluated using alpha (α) of 0.05. Significant differences in carapace thickness among measurement locations and molt stages were based on Tukey HSD post-hoc comparisons.

RESULTS

Histochemistry

Staining of intermolt, C_4, cuticle with acridine orange in a region that contained the suture and adjacent calcified cuticle (Fig. 1a) clearly differentiated the four cuticle layers, but not the suture itself (arrowhead). The epicuticle (ep) stained bright orange, whereas the exocuticle (ex) stained less intensely orange. Endocuticle (en) stained green and the membranous layer (ml) stained bright green. In this section (Fig. 1a) hypodermis (h) and muscle (m) could also be seen underneath the cuticle. Staining of a comparable region with toluidine blue allowed for differentiation of the two major layers of the cuticle. The exocuticle stained dark blue and the endocuticle light blue (Fig. 1b). There was no differentiation of the suture (arrowhead). Staining with periodic acid Schiff's (PAS) also allowed for differentiation between the two major layers of the cuticle. There was a marked distinction between exocuticle and endocuticle, the first staining dark pink and the second light pink (Fig. 1c). After amylase treatment PAS showed a less marked distinction between exocuticle and endocuticle (Fig. 1d). Most of the decrease in staining occurred in the exocuticle with the endocuticle showing little or no decrease in stain intensity. Neither treatment revealed the location of the suture (arrowheads). Paraldehyde fuchsin (PAF) stain did not differentiate suture from adjacent calcified cuticle, nor did it clearly differentiate the layers of the cuticle, although the epicuticle stained slightly darker than the other three layers (Fig. 1e). The exocuticle/endocuticle boundary was visible, but that was in great part due to the difference in density of the lamellae in the two layers. Sections stained with hematoxylin and eosin clearly differentiated the exocuticle, which stained blue and was therefore basophilic, from the

endocuticle, which stained pink and was acidophilic (Fig. 1f). Like the previous stains, H&E did not show any differential staining of the suture as compared to the adjacent calcified cuticle (arrowhead). Furthermore, no difference in staining patterns was observed whether sections were fixed in alcoholic formalin or aqueous Bouin's (data not shown). In the sections, the lamellae within the exocuticle and endocuticle could be observed and no discontinuities between the suture and the adjacent calcified cuticle were apparent. The lamellae of the suture cuticle appeared to be continuous with the lamellae of the adjacent calcified cuticle.

Lectin affinity

Of the 22 fluorescent-labeled lectins used to stain the intermolt cuticle, only three demonstrated differential binding between the suture and the adjacent cuticle. These lectins were *Lens culinaris* agglutinin (LCA), *Pisum sativum* agglutinin (PSA), and *Vicia faba* agglutinin (VFA). These three lectins revealed the suture shape to be trapezoidal (Fig. 2 a-d). The three lectins bound to the suture region of the exocuticle (arrowhead), staining it much more intensely than the adjacent exocuticle (ex). The suture region of the endocuticle (arrow), however, was more lightly stained than the adjacent endocuticle (en) in a pattern forming a wedge with sides approximately 45 degrees to each other, being narrower at the distal end where it met the exocuticle (approximately 40 μm), and wider at the proximal end, where it met the membranous layer (approximately 75 μm). In some sections (Fig. 2 c and d, and 3 c) the prisms (asterisk) in the adjacent exocuticle, especially at the proximal end where they met the endocuticle, also stained more intensely than other regions of the exocuticle, including the interprismatic septa. Sections

fixed in alcoholic formalin (Fig. 2) stained more intensely than sections fixed in aqueous Bouin's (Fig. 3 c and d). This difference in binding affinity of the lectins as a function of the fixative was most pronounced in sections stained with VFA, where the lectin did not bind to the cuticle fixed in aqueous Bouin's, thus making it undistinguishable from the unstained controls (Fig. 3 a and b). In the controls, the epicuticle (arrowhead), including setae (arrow), autofluoresced, whereas the remainder of the cuticle did not.

Scanning electron microscopy

An external and internal view of the suture, using secondary electron mode (SE), showed that there is a shallow groove in the intermolt cuticle in the region of the suture (Fig. 4 a-e, arrow), thereby making it slightly thinner than the adjacent cuticle. Externally, on the anterior ventral branchial lobe of the carapace, a series of knobs formed a ridge (arrowhead) that paralleled the suture along almost its entire length (Fig. 4 a). Unlike the cuticle surrounding the suture region, no setae were seen over the suture (Fig. 5b). The internal, or proximal, surface of the cuticle had a smooth texture, possibly due to organic matter dried on the surface. The suture was only a shallow depression, just barely below the surface of the adjacent calcified cuticle. The external and internal aspects of the suture were observed in the cuticle of intermolt crabs and five premolt stages, and there were no noticeable differences in its appearance among the different stages. In comparison, imaging with the back-scattered electron (BSE) mode indicated that the suture region (arrow) was less calcified (Fig. 4 d). That is, the cuticle adjacent to the suture was bright, forming a scalloped pattern (Fig. 4d, also seen in the SE Figure 4c). The suture had an intermediate brightness at the margins, and was completely dark (i.e.

void of BSE signal) at the center (Fig. 4d, arrow). In contrast, the margins of canals containing receptors that pass through the entire cuticle (Fig. 4 d arrowhead) seemed to be more heavily mineralized, since they were brighter. X-ray maps of calcium in both regions were consistent with this interpretation (Fig. 4 e).

Fracture surfaces of intermolt cuticle observed with the secondary electron (SE) detector of the scanning electron microscope (SEM) in cross section showed that the cuticle layers of the suture (arrow) are contiguous with those of the adjacent cuticle (Fig. 5 a, c, and d). The suture (arrow in Figure 5 a and b) was visible and had no setae. Prisms (arrow in Figure 5 c, d, e, and f) and interprismatic septa at the suture exocuticle and its vicinity were distinguishable, especially in the back-scattered electron (BSE) micrographs (Fig. 5 d and f) where the septa were brighter than the prisms, indicating they contained more calcium. Observations with the BSE mode revealed that the prisms of the exocuticle in the suture were not in-filled with calcium (Fig. 5 d). Prisms were less in-filled with calcium the farther away from the external surface of the suture, thereby forming a wedge pattern (Fig. 5 c and d). In the adjacent cuticle, farther away from the suture, the exocuticle appeared more solid, with the prisms almost completely in-filled with mineral (Fig. 5 e). However, often some portions of the prisms (arrow in Fig. 5 e) close to the interface with the endocuticle (arrowhead) were not completely in-filled. A higher magnification of the exocuticle of the suture (Fig. 5 f) showed prisms not in-filled (arrow) and septa (brighter regions) that were mineralized. No noticeable difference in the structure and mineral content between the suture region of the endocuticle and the adjacent calcified endocuticle could be detected in these fractured samples.

Geometry between the regions being observed and the back-scattered electron (BSE) or X-ray detector clearly played a role in signal intensity. For example, shadowed regions could be erroneously interpreted as less calcified regions. Therefore, the use of embedded and cut samples was appropriate for observations and analysis with BSE and X-ray modes. Observation of the embedded and cut samples with BSE mode (Figs. 6 and 7) revealed that the exocuticle of the suture (arrowhead) was less calcified than the adjacent exocuticle (ex). More specifically, the prisms were not in-filled with calcium carbonate in the region of the suture. Prisms farther away from the suture gradually were increasingly more in-filled with mineral, forming a visible wedge (* on Figure 6 e). Endocuticle at the suture (arrow) also appeared less mineralized than the adjacent endocuticle (en). It formed a wedge pattern as well, with an angle of approximately 45 degrees, narrower (approximately 40 μm) at the distal end and wider (between 100 μm and 250 μm approximately) at the proximal end. There was a noticeable difference in the width of this wedge among anterior, middle, and posterior pieces of cuticle from the same crab. In posterior pieces of cuticle the wedge was wider, measuring approximately 100 μm in the center of the endocuticle. In middle pieces the wedge measured approximately 50 μm, and in anterior pieces the wedge was about 30-40 μm wide. In crabs from later premolt stages (Fig. 7 a-f), closer to ecdysis, the suture region of the endocuticle (arrows) appeared even less mineralized and more digested at the inner portions of the cuticle in the same wedge pattern. Digestion advanced further up into the cuticle of the suture as the crab approached ecdysis (Fig. 7 b, d and f). Prior to digestion and demineralization, the suture and the adjacent cuticle's inner surface were almost on the same plane at stage C_4, with the suture just barely below the surface of the calcified

adjacent cuticle. Digestion and demineralization progressed through the premolt stages with the digestion removing the inner portions of the endocuticle across the entire cuticle, but preferentially at the suture. Digestion and demineralization followed the less calcified wedge shaped region seen in BSE micrographs (Figs. 6 and 7) forming a deeper groove and thus making the suture even thinner as compared to the adjacent cuticle (Fig. 8a). By stage D_3 virtually the entire endocuticle region of the suture was digested causing the carapace to split (not shown). This digestion and demineralization pattern was slightly different among anterior, middle, and posterior sections of each crab. The posterior section showed more pronounced demineralization and digestion than the anterior and middle sections (cf. Fig. 6e and 6f, and Fig. 7e and 7f). Posterior pieces appeared to start demineralizing and being digested earlier than the other two regions sampled, so the suture cuticle was removed to a greater extent in posterior pieces. Demineralization seemed to precede digestion of the organic matrix, resulting in a layer on the inner surface of the cuticle that was detectable in BSE images (e.g. Fig. 7c and 7e). This layer had an average atomic number closer to that of the resin than the calcified cuticle.

A difference in thickness of the cuticle was also noted among anterior, middle, and posterior regions. Cuticle region, carapace measurement location, and stage of the molt cycle each demonstrated significant effects on cuticle thickness (Fig. 8). Mean cuticle thickness was significantly lower in the suture region compared to the adjacent calcified cuticle region ($p < 0.0001$; Fig. 8a) and cuticle thickness was greatest when measured in the anterior sector of the carapace ($p < 0.0001$; Fig. 8b). The D_2 stage of the molt cycle had the lowest cuticle thickness ($p < 0.0001$; Fig. 8c). The interaction between cuticle

region and stage of the molt cycle was significant ($p = 0.0218$), with cuticle thickness varying among molt cycle stages in the suture region, but remaining constant across molt cycle stages in the adjacent calcified cuticle region.

X-ray microanalysis

Elements measured in the selected square regions were carbon, oxygen, sodium, magnesium, phosphorous, platinum (due to coating), sulfur, chloride, palladium (due to coating), and calcium. Figure 9 (a-e) shows a set of comprehensive elemental maps for calcium, magnesium, phosphorous, carbon, and oxygen distributions for an anterior piece of cuticle from an intermolt (C_4) crab. The same wedge pattern for the suture as seen in the BSE images was observed in the calcium map. A similar but much less distinct pattern was seen in the magnesium and oxygen maps. For the carbon map the pattern was the same shape but reversed, with a stronger signal in the wedge shaped suture region. For phosphorous the wedge pattern was not observed, but more of the element was present at the exocuticle non-suture (Fig. 9) than at the other regions.

Quantitative analysis of the selected cuticle regions revealed that there were significant differences in the calcium concentrations of the five regions (Table 1), except between endocuticle non-suture and exocuticle non-suture ($p > 0.05$) (Table 2), which contained the greatest concentrations of calcium. Upper endocuticle of the suture had the third greatest concentration of calcium (17.3 ± 2.9 Wt %), followed by exocuticle of the suture (13.1 ± 3.6 Wt %). Lower endocuticle of the suture had the lowest concentrations of calcium (10.4 ± 7.4 Wt %) and the highest variance, with values ranging from 0.6 to

18.3 Wt %. The region with the next highest variance was exocuticle suture (13.1 ± 3.6 Wt %) with values ranging from 7.8 to 22.1 Wt %.

There were also significantly different concentrations of magnesium among all the regions of the cuticle analyzed (Tables 1 and 2), except between upper endocuticle suture and exocuticle suture ($p > 0.05$), which had the second lowest concentrations of magnesium (Table 1). Lower endocuticle of the suture had the lowest concentration of magnesium (0.66 ± 0.45 Wt %). Exocuticle non-suture had the greatest amounts of magnesium (1.75 ± 0.24 Wt %), followed by the endocuticle non-suture (1.33 ± 0.14 Wt %).

Phosphorous concentrations were not significantly different among regions (Table 2), except for the exocuticle non-suture (Tables 1 and 2), which contained a significantly higher concentration of phosphorous than any other region (2.9 ± 0.5 Wt %). Endocuticle non-suture and exocuticle non-suture oxygen concentrations were the highest (Table 1) and did not differ significantly from each other (Table 2). Lower endocuticle of suture and exocuticle of suture had the lowest oxygen concentrations (Table 1) and did not differ significantly from each other (Table 2). Upper endocuticle of suture differed significantly from all the other regions, having intermediate oxygen concentration (23.0 ± 2.5 Wt %).

Carbon showed an opposite pattern with concentrations being the least in the endocuticle non-suture and exocuticle non-suture (Table 1), which were not significantly different from each other (Table 2). Lower endocuticle of suture and exocuticle of suture had the greatest amounts of carbon (Table 1) and did not differ significantly from each

other (Table 2). Upper endocuticle of suture differed significantly from all the other regions (Table 2), having an intermediate carbon concentration (43.6 ± 5.5 Wt %).

Since Ca/Mg and Ca/P ratios have been shown to influence the solubility of calcium salts (Stumm and Morgan, 1981), those ratios were examined in this study. Scatter plots of calcium concentrations versus magnesium concentrations (Fig. 10a) and phosphorus concentrations (Fig. 10b) revealed both the relative ratios of the two elements in different regions of the cuticle as well as the patterns of variability within those regions. Mean ratios of calcium to magnesium and phosphorous are shown in Table 3 as well as a summary of statistical analyses comparing values among the various regions. As seen in Figure 10, the distribution of values for each region analyzed clustered in separate groups for each region, forming distinct patterns. The calcium versus magnesium plot (Fig. 10a) showed that both the endocuticle non-suture and the exocuticle non-suture had comparable calcium concentrations but significantly different (Table 3a) magnesium concentrations. The exocuticle non-suture had significantly higher magnesium concentrations and thus values clustered more to the right of the plot (Fig. 10a). Ratios of calcium to magnesium for the exocuticle non-suture were the lowest (Table 3a) and were significantly different from all other regions except the lower endocuticle suture (Table 3a). The ratios of calcium to magnesium among the selected regions were highest for the endocuticle non-suture and upper endocuticle of the suture, and were not significantly different from each other (Table 3a). The upper endocuticle suture values were loosely clustered (Fig. 10a), had less calcium and magnesium than the endocuticle non-suture, but maintained the same ratio of calcium to magnesium as found in the endocuticle non-suture (Table 3a). Values for the suture region of the exocuticle and lower endocuticle

overlapped, except for a few values for lower endocuticle suture that had both low calcium and magnesium concentrations. Both regions had an intermediate Ca/Mg ratio and were not significantly different from one another (Table 3a). There was generally a positive correlation between calcium and magnesium concentrations; as the first increased, the second one increased as well (Fig. 10a). Analysis of regions containing only resin, and no cuticle, thus serving as controls, showed a tight cluster of values close to zero containing no calcium and little magnesium (Fig. 10a).

The calcium versus phosphorous plot (Fig. 10b) had patterns similar to those for the calcium versus magnesium plot (Fig. 10a). Endocuticle non-suture and exocuticle non-suture had comparable calcium concentrations, but exocuticle non-suture had a significantly greater phosphorous concentration than the endocuticle non-suture (Table 3b), thus clustering farther to the right of the plot. Exocuticle non-suture had the lowest calcium to phosphorous (Ca/P) ratio, which was significantly different from all the other regions with the exception of lower endocuticle suture (Table 3b), whereas endocuticle non-suture had the highest Ca/P ratio that was significantly different from all other regions. The remaining regions had Ca/P ratios significantly different from each other and from lower endocuticle suture and exocuticle non-suture (Table 3b). Again, a positive correlation was seen for calcium to phosphorous concentrations in the upper and lower endocuticle suture and exocuticle suture (Fig. 10b), but more so for lower endocuticle suture and exocuticle suture, which overlapped. Values for upper endocuticle suture clustered between the endocuticle non-suture values and values for the lower endocuticle suture and exocuticle suture (Fig. 10b) and were significantly different from all other regions (Table 3b). A few values for lower endocuticle suture clustered

closer to zero. Control (resin) values clustered tightly near zero, with no calcium and very little phosphorous (Fig. 10b).

DISCUSSION

This investigation has revealed several unique features of the ventral suture of the blue crab, *Callinectes sapidus*, that may contribute to creating the predetermined "lines of weakness" (Mangum, 1985) that subsequently lead to the splitting of the cuticle prior to ecdysis. While the suture morphology and the nature of its organic and inorganic components were in general very similar to that of the adjacent fully calcified cuticle, there were minor, but important, differences in the glycoproteins present and the extent of calcification. The suture was also notably thinner in the posterior portion of the carapace making it more likely to split first. Finally, the Ca/Mg ratio and Ca/P ratios in the suture differed from the adjacent calcified cuticle, which potentially made the suture more soluble than the calcified cuticle, as will be discussed below.

The histological and general histochemical techniques used in this investigation were not able to differentiate the suture from the adjacent, non-suture calcified cuticle. When stained with acridine orange, hematoxylin and eosin, periodic acid Schiff (PAS), paraldehyde fuchsin (PAF), and toluidine blue, the suture stained the same as the non-suture calcified cuticle. Since hematoxylin and eosin are sensitive to acidic and basic to neutral moieties, respectively (Presnell and Schreibman, 1997), the relative concentration of acidic and basic to neutral molecules in the layers of the calcified cuticle and suture are very similar. This is in striking contrast to the situation in the arthrodial membrane

(Williams et al., 2003), which stains very differently from the calcified cuticle. In the arthrodial membrane the region adjacent to the exocuticle is eosinophilic while the exocuticle of the calcified cuticle is strongly basophilic. The suture was also not differentiated by PAS staining, which was used to demonstrate that the pre-exuvial and post-exuvial cuticle of the arthrodial membrane was contiguous with the exocuticle and endocuticle of the calcified cuticle (Williams et al., 2003). The PAS reaction is dependant on sugars with adjacent hydroxyls reacting with Schiff's reagent after being oxidized to dialdehydes with periodic acid (Thompson, 1966; Presnell and Schreibman, 1997). The inability of PAS to differentiate the suture from the adjacent calcified cuticle indicates that any differences in the concentration of these moieties within the suture were so slight as to be undetectable. When sections were treated with amylase, PAS staining was noticeably decreased in the exocuticle, suggesting that molecules containing β-1,4-glucose moieties might be present. However, the location of the suture region was not revealed by amylase treatment either.

Staining with paraldehyde fuchsin (PAF) reveals sulfhydryl-containing molecules in tissue sections (Gomori, 1950). Such sulfhydryl-containing molecules have been localized in bovine growth plate by Byers et al. (1997) and in cementum and dentine by McKee et al. (1996), where they have been suggested to have a role in mineralization. Both the exocuticle and endocuticle stained moderate to lightly with PAF, with little difference between the two layers. Furthermore, the suture was not detectable, suggesting that while sulfhydryl-containing molecules might represent a minor component of the cuticle, they don't seem to contribute to any differences between the suture and the adjacent calcified cuticle.

Acridine orange is a fluorescent cationic dye that has been used to clearly differentiate all four layers of the cuticle in *Callinectes sapidus*, supposedly binding to glycoproteins or glucosaminoglycans (Marlowe and Dillaman, 1995). The metachromatic fluorescence demonstrated by the dye in this application seems to indicate variable concentrations of those molecules in the different layers of the cuticle. The inability of this stain to differentiate the suture from the adjacent calcified cuticle would once again suggest that any differences in these moieties between the two regions are so slight as to be undetectable.

Toluidine blue buffered to pH 9.0 is a general stain that will bind to molecules with an isoelectric point below 9.0, making it a useful histological stain for both chitin and a wide range of cytoplasmic proteins (Thompson, 1966; Presnell and Schreibman, 1997). While this stain bound much more intensely to the exocuticle, it was not able to differentiate the suture from the surrounding calcified cuticle.

In summary, the stains used in this investigation only identified categories of molecules within the cuticle, and while they were capable of differentiating individual layers within the cuticle, none was able to differentiate the suture from the surrounding calcified cuticle. Furthermore, the major structural features of the cuticle, namely the thickness and arrangement of the lamella, gave no clue as to the location of the suture. In the puparium cap of the insect *Elenchus tenuicornis*, Kathirithamby et al. (1990) have described the line of weakness as having lamellae with an "open texture" as compared to the adjacent cuticle with densely staining and compact lamellae. They further suggested that the open texture was due to the absence of tanning in the line of weakness. The absence of any difference of lamellar density and thickness in the suture of the blue crab

suggests that there is little difference in composition or tanning of the two regions. While tanning in crustaceans has been suggested by several authors (Dennell, 1947; Summers, 1967; Summers, 1968; Vacca and Fingerman, 1975; Roer and Dillaman, 1993), evidence for the timing or presence of this process in the various regions of the cuticle has not been as well documented as in other arthropods (Hackman, 1984). Taken together, these histochemical and anatomical observations indicate that the structure and general composition of the suture and adjacent calcified cuticle are virtually identical.

Lectins are a diverse group of molecules that have binding affinities for particular carbohydrate moieties. While the specificity of individual lectins can vary considerably, they have proven useful as histochemical probes (Leiner et al., 1986; Spicer and Schulte, 1992). Marlowe et al. (1994) used a battery of 21 different lectins to characterize the composition of the cuticle of *Callinectes sapidus* at various stages of the molt cycle. Of this original battery of 21 lectins, 19 showed no difference between suture and adjacent calcified cuticle, suggesting a quite similar proteoglycan and glycoprotein content. However, two lectins from the original battery (LCA and PSA), as well as VFA, an additional lectin not used by Marlowe et al. (1994), differentiated between the suture and the adjacent calcified cuticle. The suture was seen as a trapezoidal wedge whose boundaries were revealed by more intense staining in the exocuticle of the suture and by reduced staining in the endocuticular region.

All three of these lectins have been described as binding to fucosylated α-N-acetylglucosamine with mannose dendrimers (Debray et al., 1981; Young et al., 1996), and therefore indicate the presence of glycoproteins containing these types of oligosaccharides at the sites of intense binding, namely, the exocuticle of the suture and

some prisms in the vicinity of the suture. The general binding pattern was the same for the three lectins, but there were some differences in intensity, with VFA binding less intensely than the other two lectins. The differences observed in binding intensity by the three lectins may have been due to steric hindrance, differences in the size of the lectin conjugates, or the quantity of similar, but slightly different lectin-binding moieties. In addition, it was also shown in this study that fixation with alcoholic formalin favored the retention of the proteoglycans and glycoproteins of interest. Similar results were noted by Marlowe et al. (1994), who also noted intense binding of most lectins in tissue samples fixed in alcoholic formalin. Marlowe et al. (1994) also noted intense staining after fixation with Rossman's fluid, which is also referred to as alcoholic Bouin's. Fixation in aqueous Bouin's, which was used in this study, did not result in similar staining. This suggests that preservation of the oligosaccharides bound by the three lectins is more a function of the alcohol in the fixative than the presence of picric acid, which is the other major element shared by both types of Bouin's fixative.

If the moieties bound by LCA, PSA and VFA are related to the inhibition of mineralization, the observed staining patterns would predict that the exocuticle of the suture would be much less mineralized than the adjacent calcified exocuticle, but that the endocuticle of the suture would be more calcified than the adjacent endocuticle of the calcified cuticle. However, this assumes that calcification in the exocuticle and endocuticle is identical and that mineralization is regulated in the same manner by the same set of molecules. In fact, calcification in the two major layers is distinctly different. Calcification of the exocuticle occurs after ecdysis on a preformed matrix whereas endocuticle matrix is produced after ecdysis and mineralized as it is deposited (Green and

Neff, 1972; Hegdahl et al., 1977a and 1977b). Exocuticle calcification has two phases. The first phase involves the mineralization of the interprismatic septa, which starts at the outer and inner boundaries of the exocuticle and then moves towards the middle of the exocuticle (Giraud-Guille, 1984a; Hequembourg, 2002). The initial mineral phase is amorphous calcium carbonate, which later changes into a more stable form of calcium carbonate, calcite (Hequembourg, 2002; Dillaman et al., 2001). The second phase involves infilling of the prisms with mineral. The prisms fill first at the outer exocuticle boundary and mineralization then proceeds inwards (Hequembourg, 2002). The glycoproteins bound by LCA, PSA and VFA may possibly be responsible for regulating the first or second phase of calcification in the exocuticle of the suture. For example, Coblentz et al. (1998) suggested that the removal of glycoproteins after ecdysis was necessary for calcification to occur in the exocuticle. The presence of the LCA-, PSA- and VFA-binding glycoproteins in the suture exocuticle of intermolt crabs may indicate that because the glycoproteins were not removed, the cuticle was not calcified. The same interpretation could be extended to the regions of the prisms close to the endocuticle, but outside the suture, that bound the three lectins.

The vast majority of the lectins used indicated that the carbohydrate composition of the suture is more like than unlike the adjacent calcified cuticle, thereby reinforcing the histology and histochemistry results. However, the three lectins LCA, PSA, and VFA were useful for identifying the suture. Furthermore, it is possible that the minor difference in glycoprotein content at the suture may be responsible for making it more susceptible to molting fluid.

The suture at intermolt is visible to the unaided eye due to the presence of a groove observed internally and externally, the absence of setae on the exterior of the carapace over the suture, and the presence of a knobbed ridge paralleling the suture on the external surface. Since the groove makes the suture thinner, one may assume that it is weaker than the adjacent calcified cuticle. The observed decreases in thickness varied with molt stage and location on the carapace, i.e. the suture was thinnest at late premolt and at the posterior aspect of the carapace. All these characteristics (being thinner than adjacent calcified cuticle, being thinnest at late premolt, and being thinnest at posterior) make the suture mechanically weaker thereby directing a fracture in a specific location, much like scoring glass (Vogel, 1988). The phenomenon that puts the old cuticle under tension is the rising internal pressure due to the water uptake by the crab prior to ecdysis (Passano, 1960; Green and Neff, 1972; Mangum et al., 1985). The suture, therefore, preferentially fails (or splits) first at the posterior end of the carapace, so that the crab can crawl out of the old shell or exuvium.

The BSE and X-ray analysis showed exactly the same trapezoidal morphology for the suture as the lectin staining revealed. In a developmental sense, this trapezoidal, wedged-shaped pattern suggests that the epithelium depositing the suture is not a fixed number of cells. Since mitosis in the hypodermis precedes the deposition of the cuticle, from D_1 to C_3 epithelial cells at the margin of the suture must be differentiating from those forming non-suture calcified cuticle into suture-forming epithelia, in much the same way as previously noted by Williams et al. (2003) in their investigation of the epithelium forming the arthrodial membrane of the blue crab. Furthermore, since the suture trapezoidal shape varies from anterior to posterior regions of the carapace, the pattern of

cell differentiation also varies spatially. Since the structure of the non-suture calcified cuticle and the suture appear to be so similar, this differentiation may involve simply turning on or off a few genes.

In back-scattered electron (BSE) images the signal is brighter when higher atomic number elements are present (Murphy, 2001). The observed brighter regions in the cuticle were therefore due to mineralization. This was verified by X-ray mapping. In the exocuticle of the suture the bright BSE signal indicated that only the interprismatic septa (IPS) were mineralized. The prisms were clearly not mineralized in the exocuticle region of the suture and resembled 8hr postmolt exocuticle described by Hequembourg (2002), for mineralized cuticle. This indicates that the initial phase of calcification in the suture exocuticle, the mineralization of the IPS, was not different from that of non-suture exocuticle. However, the second phase of calcification in the suture, the in-filling of the prisms, was presumably arrested in early postmolt. This appears to be a permanent inhibition of mineralization because when the surface of the suture in fully mineralized intermolt crabs was examined by BSE the suture appeared dark, thus much less calcified than the adjacent cuticle. This was also verified by X-ray mapping. While grey boundaries were visible in the BSE images due to the trapezoid shape of the suture, the depth of the endocuticle exceeded the depth of penetration of the electron beam, so the center of the suture looked uniformly black.

Back-scattered electron (BSE) images of the endocuticle as well as X-ray maps revealed that there was slightly less calcium in the suture than in the adjacent calcified cuticle. This is inconsistent with the previously stated suggestion that the degree of inhibition of mineralization is directly related to the intensity of lectin staining with LCA,

PSA and VFA. Rather, these observations suggest that these lectins are binding more than one glycoprotein, and that those glycoproteins, while having similar oligosaccharides, would have to have opposite roles, one being an inhibitor of mineralization and the other a promoter. This concept of molecules, including glycoproteins, serving as both inhibitors and promoters of crystal nucleation is not new and has been suggested to occur in many calcifying systems (Crenshaw, 1982; Addadi and Weiner, 1985; Wheeler et al., 1988; Gunthorpe et al., 1990). Addadi and Weiner (1985) stated that nucleation occurred when some proteins were attached to a solid substrate, such as an organic matrix, whereas inhibition occurred when some proteins were not attached, but in solution and interacting with the formed crystal.

Secondary electron (SE) images supported the information from back-scattered electron (BSE) and X-ray maps. The matrix fibers of the suture exocuticle were covered with mineral in the interprismatic septa (IPS), but in the prisms the fibers were clearly visible. The fibers/lamellae were contiguous between the suture and adjacent calcified cuticle, thereby verifying the results of the general histological and histochemical stains. There was no departure from the morphology of the calcified adjacent cuticle. While the empty prisms allowed one to determine the boundaries of the suture in the exocuticle in the SE mode, the same was not true for the endocuticle because the difference in the degree of mineralization was so slight in the suture as compared with the adjacent calcified cuticle as to make them indistinguishable. Taken together the SE images would suggest that the type and ultrastructure of the mineral is not different in the suture, but that either one phase is omitted (in the exocuticle) or that the degree of mineralization is slightly altered (in the endocuticle).

Those differences in the elemental composition between regions of the suture and the adjacent calcified cuticle were quantified with X-ray microanalysis. The major observation is that the suture is less mineralized than the adjacent calcified cuticle. In addition, the ratio of minor elements to calcium differed significantly between the suture and adjacent calcified cuticle. Ratios of minor elements, especially magnesium and phosphorous, in calcified structures have been examined in a variety of structures from bone to shells, and speculations have been made on the effects these minor elements have on the crystal structures and solubility (Giraud-Guille and Quintana, 1982; Crenshaw, 1982; Compère et al., 1993; Raz et al., 2002). All regions of the suture had a significantly lower relative concentration of magnesium as compared to the adjacent calcified cuticle. As described by Stumm and Morgan (1981), high magnesium calcites have a lower solubility, which would render the calcified cuticle less soluble than the suture, therefore making the suture more susceptible to digestion by molting fluid. There may be multiple roles for magnesium and phosphate in the cuticle. It has been reported that both magnesium (Aizenberg et al., 2001) and phosphorus (Levi-Kalisman et al., 2000) stabilize the amorphous calcium carbonate in ascidian spicules. Since amorphous calcium carbonate is also present in non-suture calcified cuticle (Lowenstam and Weiner, 1989; Vinogradov, 1953; Dillaman et al., 2001), it is possible that the blue crab may be making slight modifications in the mechanisms for regulating mineralization in order to effect a difference in mineral solubility. The preferential thinning of the suture during premolt appears to be due to demineralization followed by partial digestion of the organic matrix. The mineral concentration seemed to gradually decline throughout premolt stages, leaving an organic layer on the inner surface of the cuticle, referred to as ‘ecdysial

membrane' by Compère et al. (1998). Measurements for the lower endocuticle suture were taken where this gradual demineralization of the suture first occurred, so the lower endocuticle suture displayed a wide range of calcium concentrations. This range would presumably reflect the transition from mineralized to unmineralized matrix. A similar distribution of calcium concentrations in the exocuticle suture suggests a similar process may be occurring.

In summary, the first hypothesis, that the ventral suture line morphology does not vary from that of the calcified cuticle surrounding it, was not supported with respect to thickness and external morphology. However, the hypothesis was supported with respect to internal morphology, particularly the structure of the lamellae in the suture, which were indistinguishable from and contiguous with those in the calcified cuticle. Consequently, the suture in *Callinectes sapidus* seems very different from the descriptions (albeit limited) of suture regions in insects (Chapman, 1982; Kathirithamby et al., 1990; Hadley, 1994). The second hypothesis, that the organic matrix of the suture line of crustaceans has the same composition as the adjacent calcified cuticle was also supported in great measure, with several general histological and histochemical stains being unable to differentiate the two regions. However, while lectin histochemistry for the most part also demonstrated similarities, three lectins out of the 22 were able to clearly differentiate the suture region. The binding by the three lectins, *Lens culinaris* agglutinin, *Pisum sativum* agglutinin and *Vicia faba* agglutinin, suggested a group of glycoproteins with similar oligosaccharides that may have very different effects on calcification in the two major calcified layers of the suture. In the exocuticle the glycoproteins may be responsible for blocking the second phase of calcification whereas

in the endocuticle they may be responsible for normal calcification. The third hypothesis, that the mineral content of the suture does not vary from that of the surrounding calcified cuticle, was clearly rejected. The suture exocuticle and endocuticle were both significantly less calcified than the adjacent calcified cuticle, thereby potentially making it easier to dissolve prior to ecdysis. In addition, the suture also had a higher calcium to magnesium and calcium to phosphate ratio than the adjacent calcified cuticle, making it potentially more soluble and therefore more susceptible to digestion by molting fluid. The fourth hypothesis was also rejected. The suture did vary in dimensions among locations. The combination of wider and thinner suture at the posterior portion of the dorsal carapace make it more susceptible to digestion, allowing the posterior portion of the suture to be digested first and allowing the crab to escape its old carapace. Taken altogether, the subtle differences in matrix composition, mineral concentration and composition, and decreased thickness in prescribed regions make the suture less stable and mechanically weaker, thus predisposing it to fail and thereby assuring successful ecdysis.

Figure 1. Light micrographs of intermolt (C_4) cuticle containing the suture (arrowhead) stained with acridine orange (a), toluidine blue (b), periodic acid Schiff (c), amylase-treated as control for periodic acid Schiff (d), paraldehyde fuchsin (e), and hematoxylin and eosin (f). en, endocuticle; ep, epicuticle; ex, exocuticle; h, hypodermis; m, muscle; ml, membranous layer.

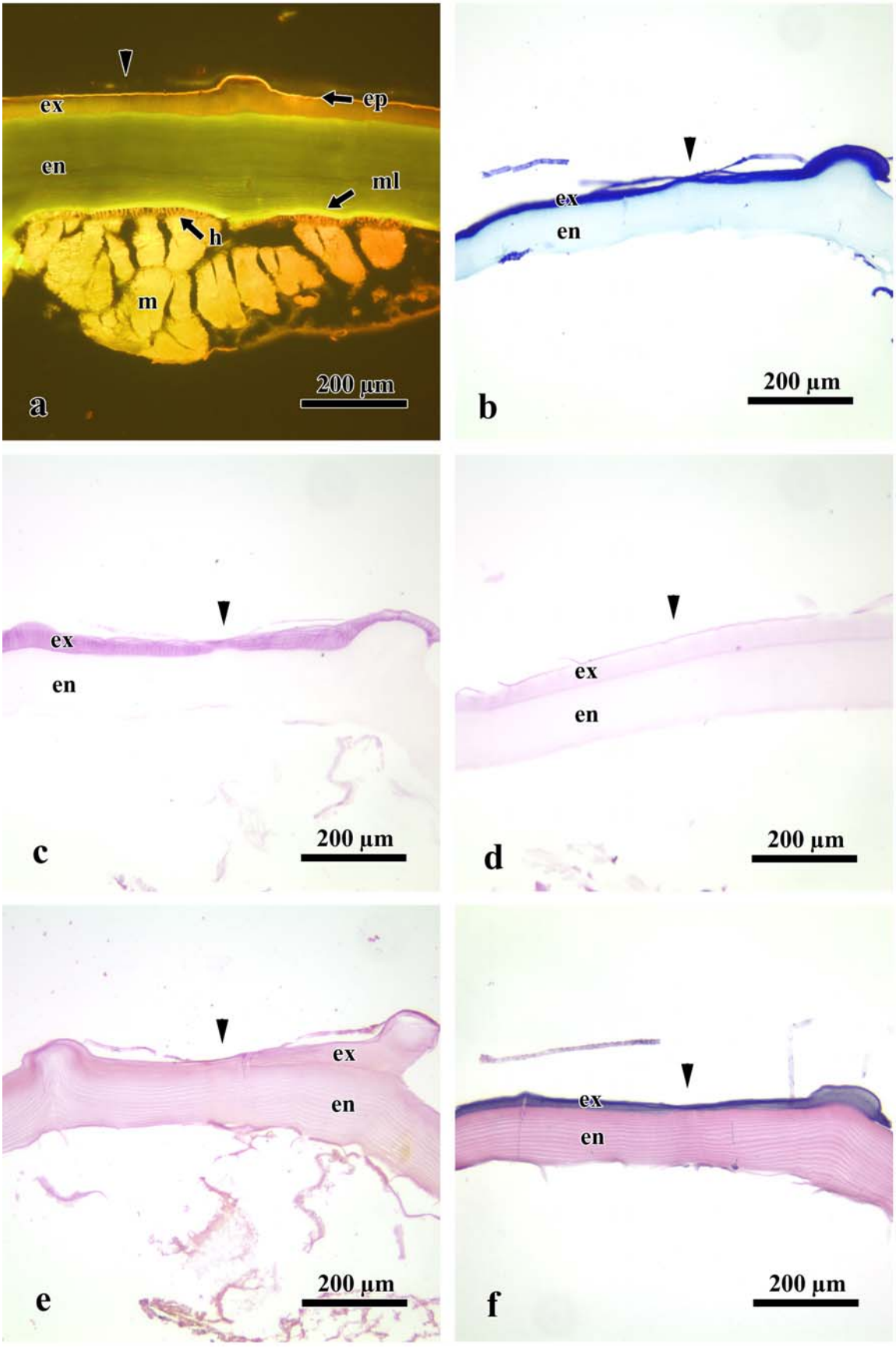
ex
ep
en
ml
h
m
200 µm
a
ex
en
200 µm
b
ex
en
200 µm
c
ex
en
200 µm
d
ex
en
200 µm
e
ex
en
200 µm
f

Figure 2. Fluorescence images of intermolt cuticle regions containing the suture, fixed in alcoholic formalin, and stained with (a) *Lens culinaris* agglutinin (LCA), (b and c) *Pisum sativum* agglutinin (PSA), or (d) *Vicia faba* agglutinin (VFA). Arrows, suture region in the endocuticle; arrowheads, suture region in the exocuticle; *, prisms; en, endocuticle; ex, exocuticle.

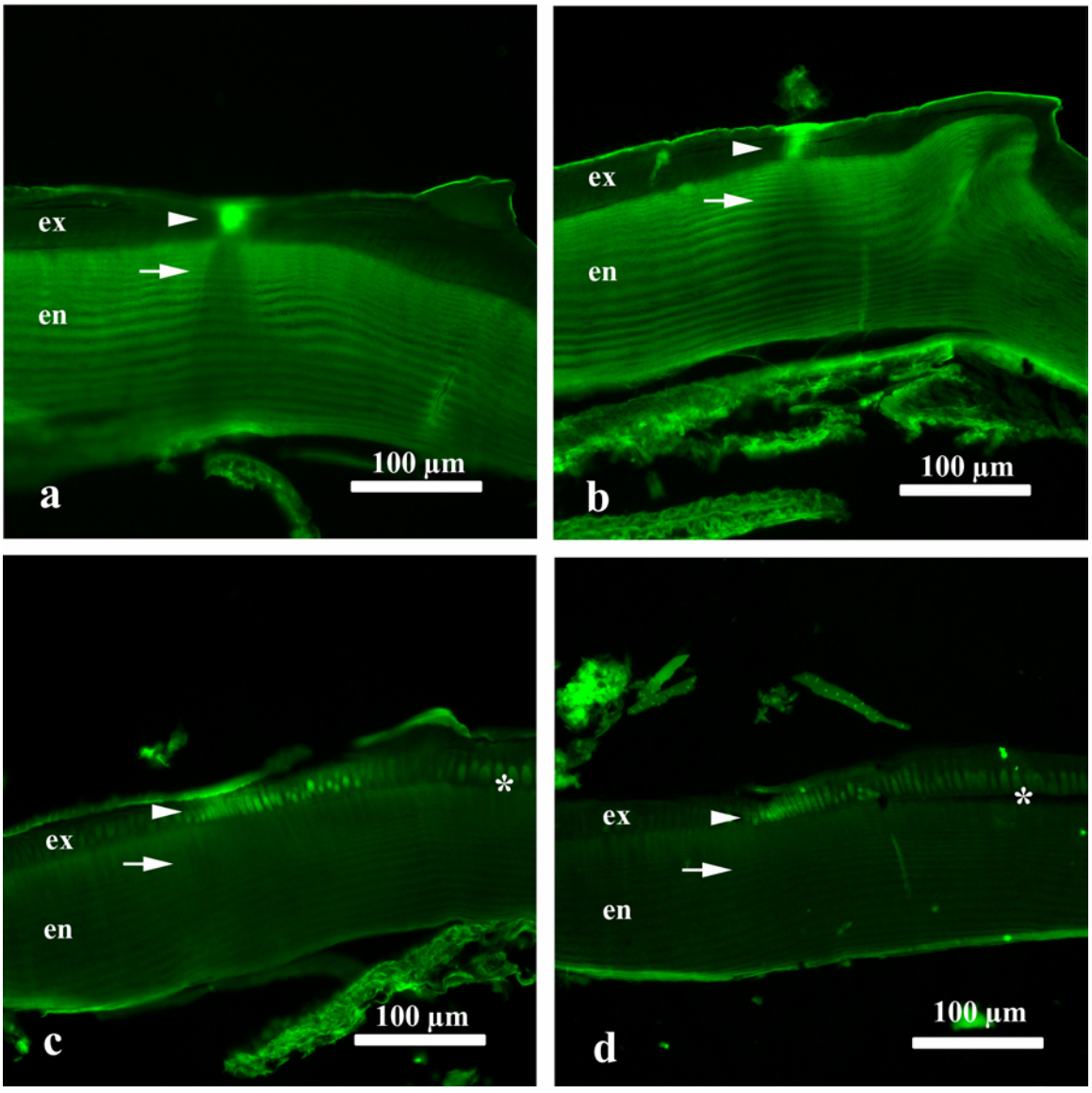
ex
en
100 µm
a
ex
en
100 µm
b
ex
en
100 µm
c
ex
en
100 µm
d

Figure 3. a & b. Fluorescence images of cuticle regions containing the suture, fixed in (a) alcoholic formalin or (b) Bouin's, and not stained to serve as controls. *, setae; arrowheads, epicuticle. c & d. Fluorescence images of cuticle regions containing the suture, fixed in Bouin's, and stained with (c) *Lens culinaris* agglutinin (LCA) or (d) *Pisum sativum* agglutinin (PSA). Arrows, suture region in the endocuticle; arrowheads, suture region in the exocuticle; *, prisms; en, endocuticle; ex, exocuticle.

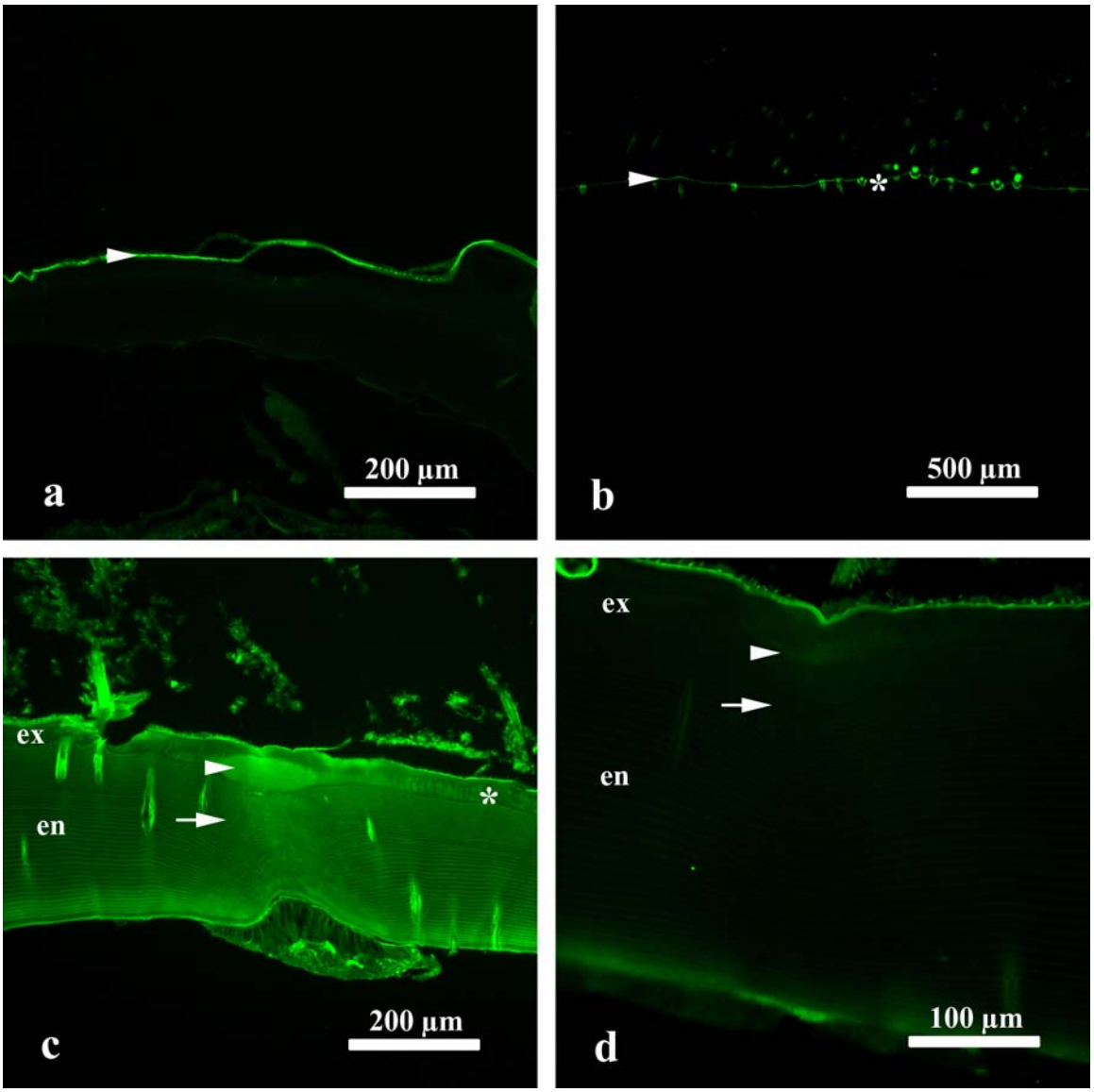
a
200 µm
b
500 µm
ex
en
c
200 µm
ex
en
d
100 µm

Figure 4. SEM micrographs of the region of the suture (arrows) of an intermolt cuticle showing external (a, c, and d) and internal (b) surfaces. Micrographs a, b and c are SE, d is BSE, and e is a calcium X-ray map. Micrographs a and b are from the anterior aspect of the carapace, whereas c, d, and e are from the posterior. Externally, a series of knobs forming a ridge (arrowhead in a) parallels the suture, except at the posterior aspect of the carapace (c, d, and e). The margin of canals containing receptors (arrowhead in d and e) seems to have a higher atomic number than the surrounding cuticle.

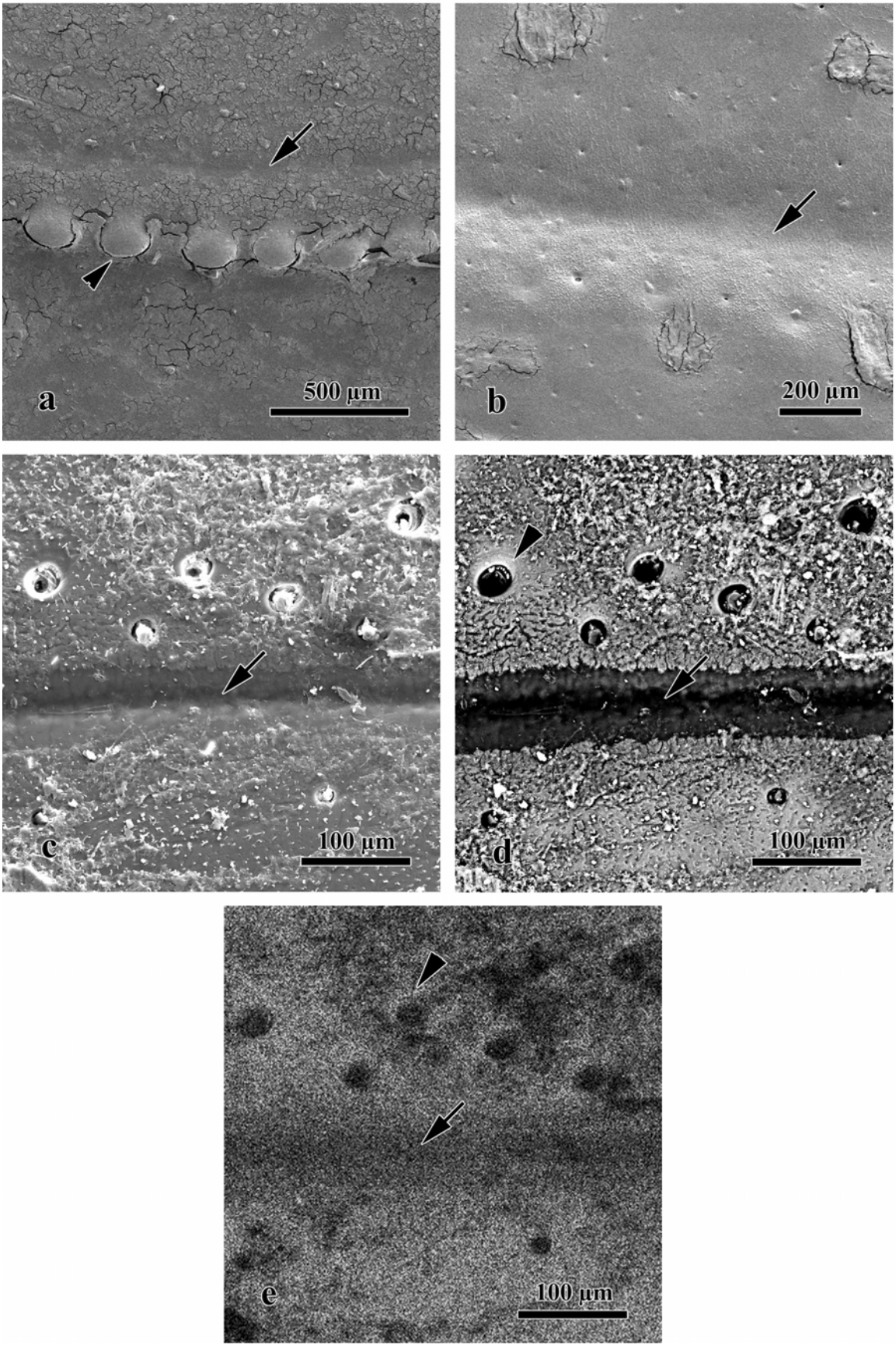
a
500 µm
b
200 µm
c
100 µm
d
100 µm
e
100 µm

Figure 5. SEM micrographs of fractured samples of intermolt crabs from posterior (a-e) and anterior (f) sectors of the carapace. Micrographs a, b, c, and e are SE, d and f are BSE. a & b. Exocuticle containing the entire suture (arrow). c & d. Details of the right margin of the suture. e. Calcified cuticle adjacent to suture. f. High magnification of the exocuticle in mid-suture of b. Arrows (a and b), suture; arrows (c, d, e, and f), prisms; arrowhead, interface of exocuticle and endocuticle.

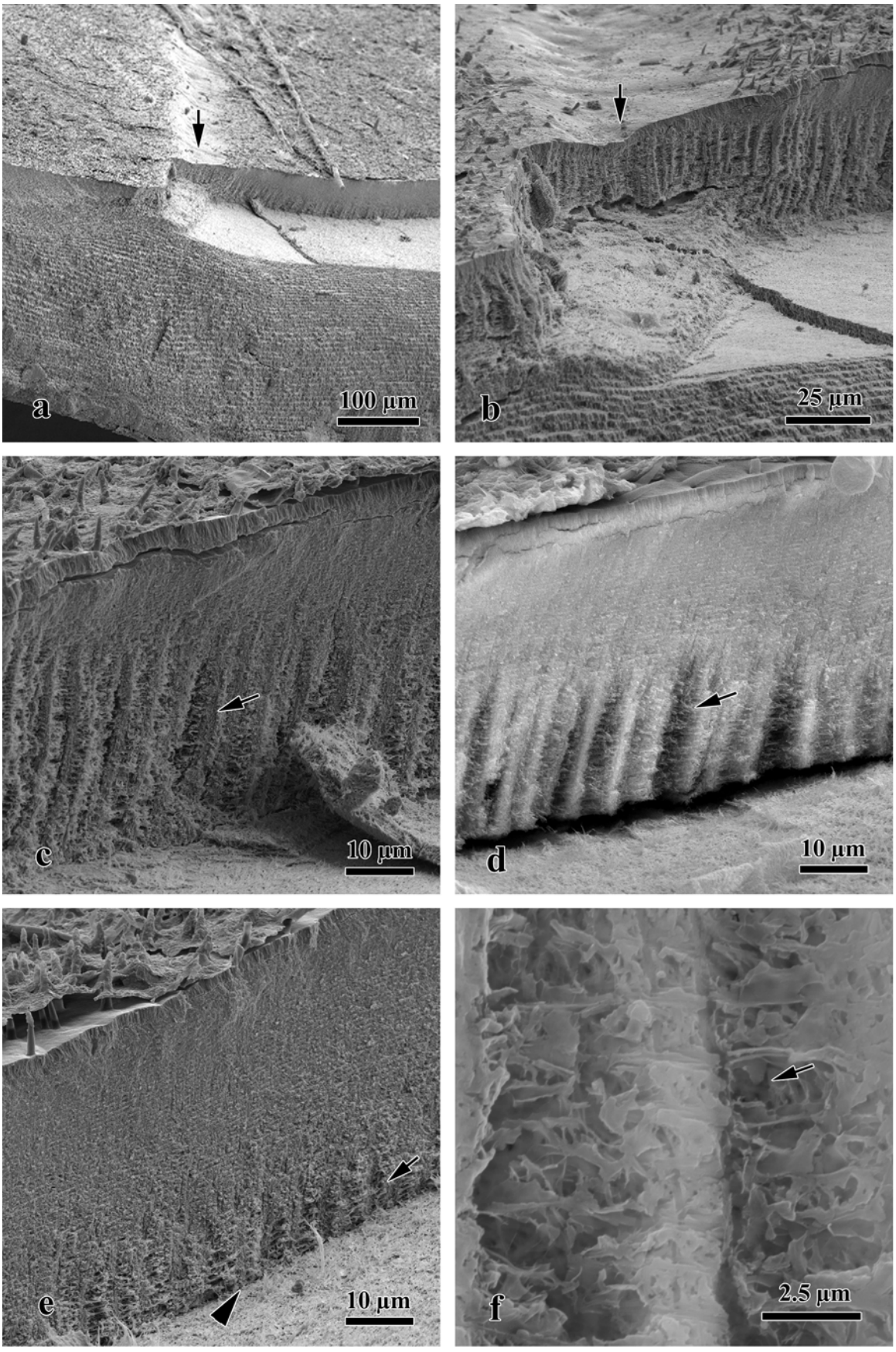
a
100 µm
b
25 µm
c
10 µm
d
10 µm
e
10 µm
f
2.5 µm

Figure 6. BSE micrographs of embedded and cut samples containing the suture of crabs in intermolt and D_1'' stages. Numbered boxes in (a) exemplify the regions that were analyzed in each sample: 1. Endocuticle non-suture, 2. Lower endocuticle suture, 3. Upper endocuticle suture, 4. Exocuticle suture, and 5. Exocuticle non-suture. Arrows, suture region of the endocuticle; arrowheads, suture region of the exocuticle; *, prisms; en, endocuticle; ex, exocuticle.

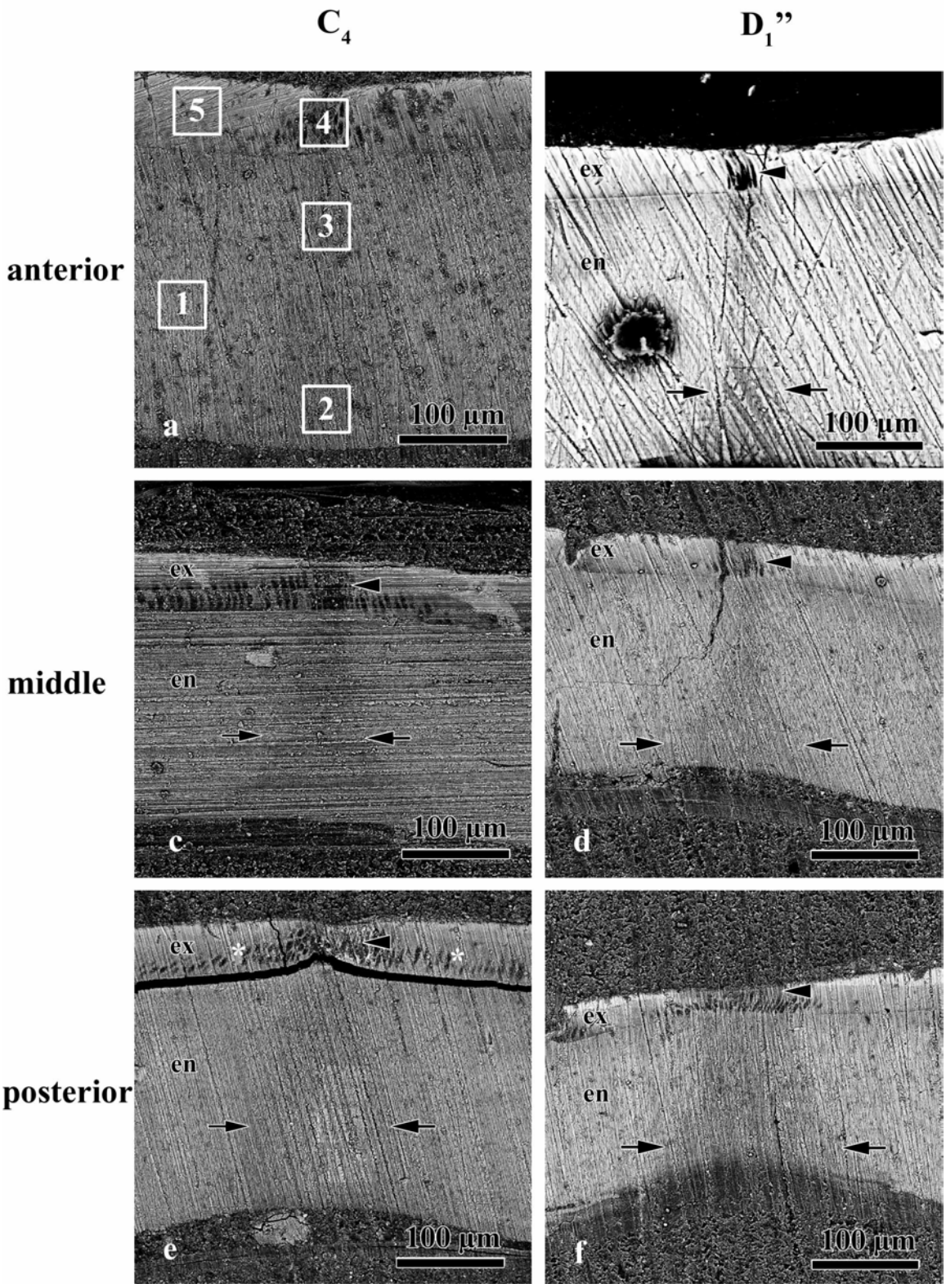
C4
D1"
anterior
middle
posterior
5
4
3
1
2
a
100 µm
ex
en
100 µm
ex
en
c
100 µm
ex
en
d
100 µm
ex
en
e
100 µm
ex
en
f
100 µm

Figure 7. BSE micrographs of embedded and cut samples containing the suture of crabs in early and late D_2 stages. Arrows, suture region of the endocuticle; arrowheads, suture region of the exocuticle; en, endocuticle; ex, indicates exocuticle.

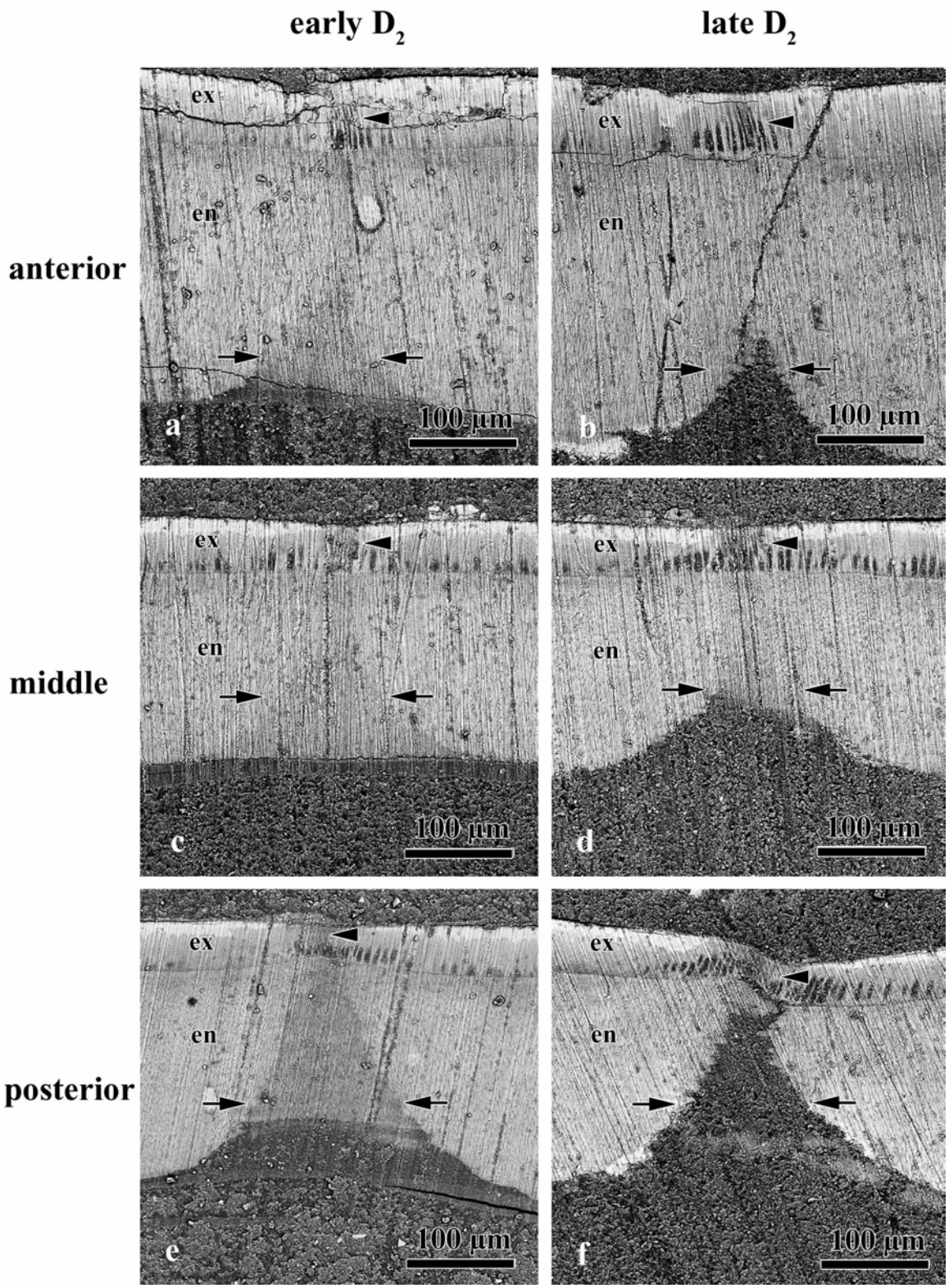
early D_2
late D_2
anterior
middle
posterior
ex
en
100 µm
a
b
c
d
e
f

Figure 8. Mean cuticle thickness (μm) (± SEM) versus (a) region of the cuticle; (b) carapace location; and (c) stage of the molt cycle. Sample size = 66. Lower case letters (a or b) above bars in panels b and c indicate significant differences in carapace thickness among measurement locations and molt stages based on Tukey HSD post-hoc comparisons.

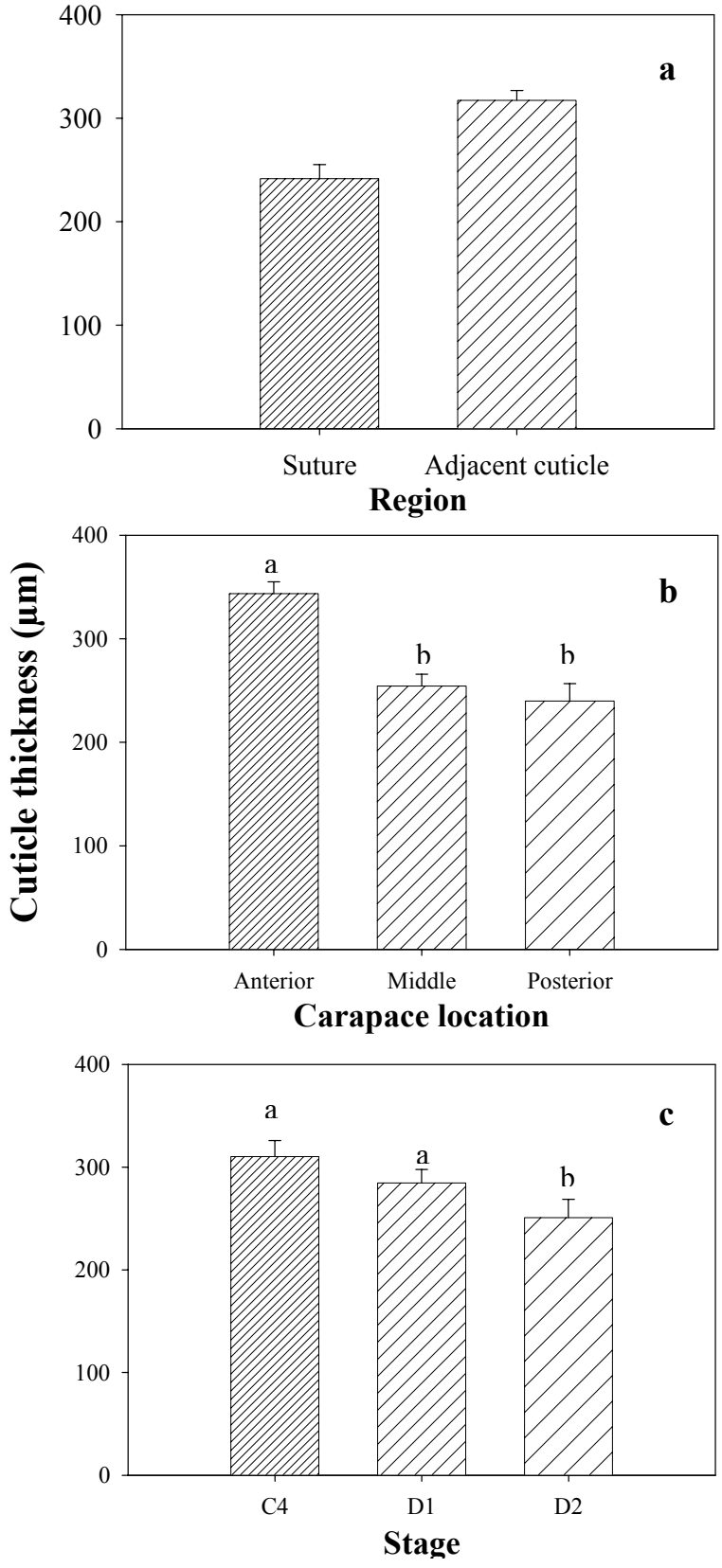
400
300
200
100
0
a
Suture
Adjacent cuticle
Region
Cuticle thickness (µm)
400
300
200
100
0
a
b
b
b
Anterior
Middle
Posterior
Carapace location
400
300
200
100
0
a
a
b
c
C4
D1
D2
Stage

Figure 9. X-ray maps of an embedded anterior piece of cuticle from an intermolt crab containing the suture. Elements mapped were (a) calcium, (b) magnesium, (c) phosphorous, (d) carbon, and (e) oxygen. Arrows, suture region of the endocuticle; arrowheads, suture region of the exocuticle; en, endocuticle; ex, exocuticle.

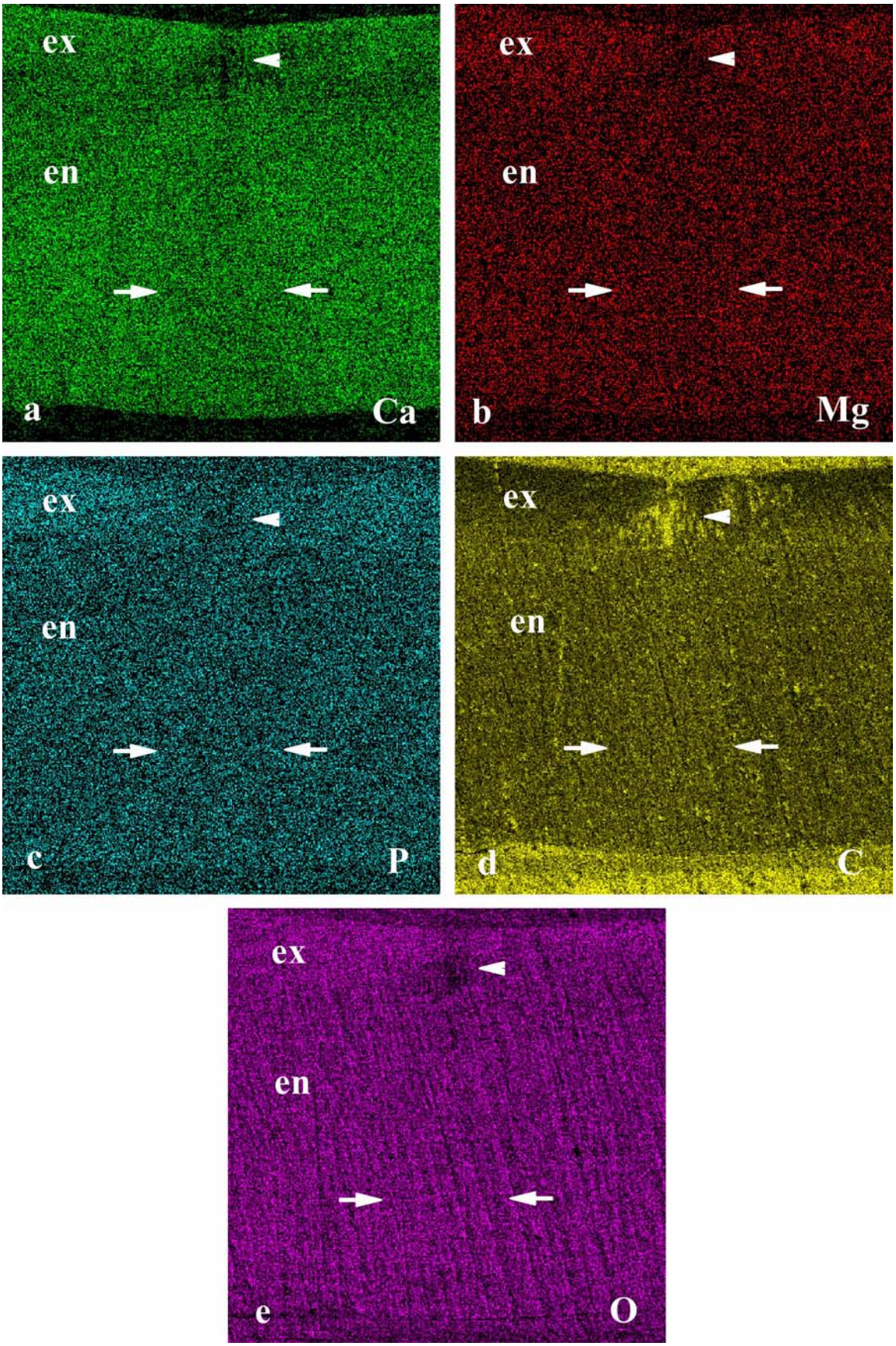
ex
en
a
Ca
ex
en
b
Mg
ex
en
c
P
ex
en
d
C
ex
en
e
O

Figure 10. Plots of calcium concentrations (Wt %) among cuticle regions against magnesium (a) and phosphorous (b) concentrations (Wt %).

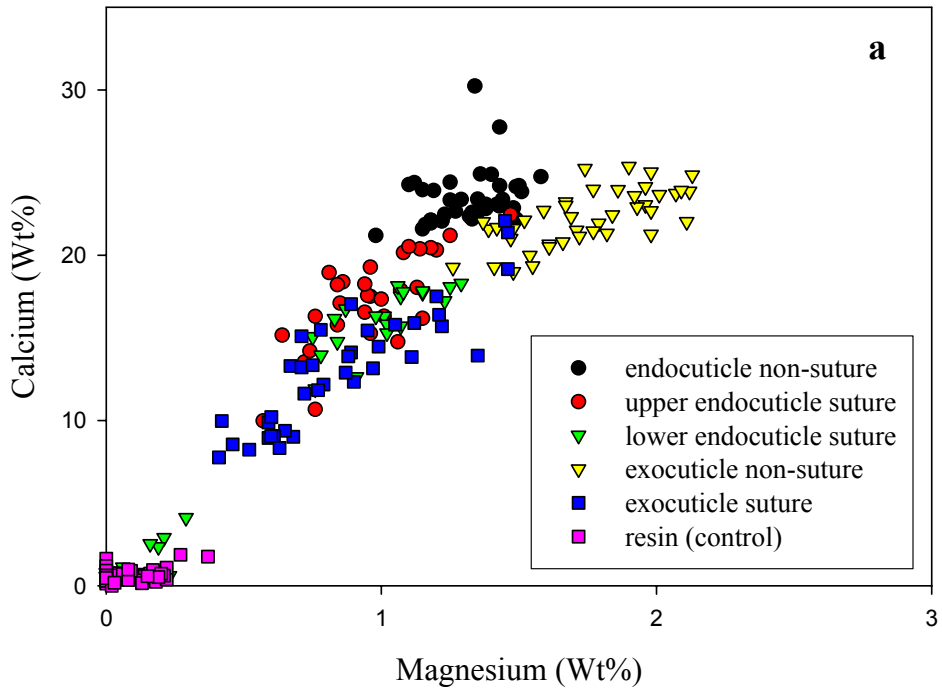
a
Calcium (Wt%)
Magnesium (Wt%)
0
10
20
30
0
1
2
3
endocuticle non-suture
upper endocuticle suture
lower endocuticle suture
exocuticle non-suture
exocuticle suture
resin (control)

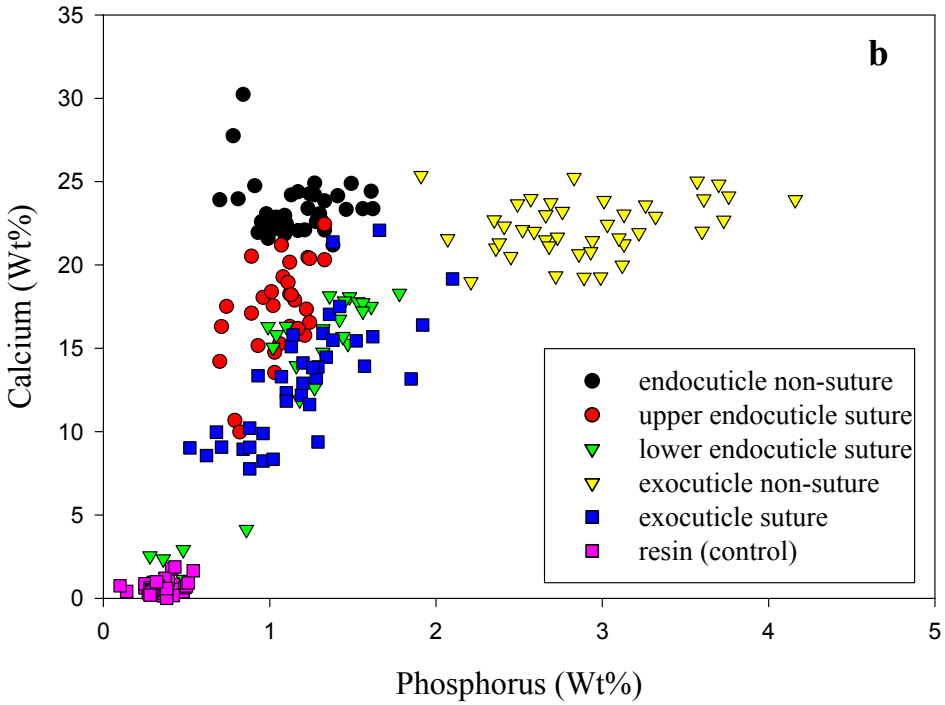
b
Calcium (Wt%)
Phosphorus (Wt%)
0
5
10
15
20
25
30
35
0
1
2
3
4
5
endocuticle non-suture
upper endocuticle suture
lower endocuticle suture
exocuticle non-suture
exocuticle suture
resin (control)

Table 1. Concentration (Wt%) of elements in suture and adjacent cuticle regions for molt stages $C_4 - D_3$ (mean ± S.D.).

		Elements (Wt%)				
Regions	**N**	**Ca**	**Mg**	**P**	**O**	**C**
Endocuticle non-suture	38	23.4 ± 1.7	1.31 ± 0.14	1.17 ± 0.23	27.3 ± 1.5	33.2 ± 2.4
Upper endocuticle suture	30	17.3 ± 2.9	0.96 ± 0.20	1.05 ± 0.18	23.0 ± 2.5	43.6 ± 5.5
Lower endocuticle suture	33	10.4 ± 7.4	0.66 ± 0.45	0.99 ± 0.50	18.6 ± 6.7	55.2 ± 15
Exocuticle non-suture	41	22.3 ± 1.7	1.75 ± 0.24	2.90 ± 0.50	28.8 ± 1.8	30.4 ± 3.5
Exocuticle suture	38	13.1 ± 3.6	0.86 ± 0.29	1.21 ± 0.35	19.7 ± 3.1	51.4 ± 6.8

Table 2. Statistical analysis of elemental concentrations among regions of the cuticle (see Table 1 for values). ***, significantly different ($p < 0.001$); ** significantly different ($p < 0.005$); * significantly different ($p < 0.05$); N.D., not significantly different.

regions\elements	**Ca**	**Mg**	**P**	**O**	**C**
endocuticle non-suture vs. upper endocuticle suture	↑ ***	↑ ***	N.D.	↑ ***	↓ ***
endocuticle non-suture vs. lower endocuticle suture	↑ ***	↑ ***	N.D.	↑ ***	↓ ***
endocuticle non-suture vs. exocuticle non-suture	N.D.	↓ ***	↓ ***	N.D.	N.D.
endocuticle non-suture vs. exocuticle suture	↑ ***	↑ ***	N.D.	↑ ***	↓ ***
upper endocuticle suture vs. lower endocuticle suture	↑ ***	↑ ***	N.D.	↑ ***	↓ ***
upper endocuticle suture vs. exocuticle non-suture	↓ ***	↓ ***	↓ ***	↓ ***	↑ ***
upper endocuticle suture vs. exocuticle suture	↑ ***	N.D.	N.D.	↑ **	↓ ***
lower endocuticle suture vs. exocuticle non-suture	↓ ***	↓ ***	↓ ***	↓ ***	↑ ***
lower endocuticle suture vs. exocuticle suture	↓ *	↓ *	N.D.	N.D.	N.D.
exocuticle non-suture vs. exocuticle suture	↑ ***	↑ ***	↓ ***	↑ ***	↓ ***

Table 3. Mean values for the ratios of Ca/Mg (a) and Ca/P (b) at the different cuticle regions. Statistical analysis of the ratios among regions is summarized below the mean values. ***, significantly different ($p < 0.001$); ** significantly different ($p < 0.005$); * significantly different ($p < 0.05$); N.D., not significantly different.

a

	Ratios (Mean ± SD)	**Regions** ENS	UES	LES	EXNS	EXS
Regions	ENS	18 (±1.9)				
	UES	N.D.	18.2 (±2.5)			
	LES	***	***	14.5 (±4.4)		
	EXNS	***	***	N.D.	12.9 (±1.3)	
	EXS	**	**	N.D.	***	15.8 (±2.7)

b

	Ratios (Mean ± SD)	**Regions** ENS	UES	LES	EXNS	EXS
Regions	ENS	21.0 (±5.3)				
	UES	***	16.7 (+±3.0)			
	LES	***	***	8.7 (±4.7)		
	EXNS	***	***	N.D.	7.9 (±1.4)	
	EXS	***	***	*	***	11.2 (±2.3)

LITERATURE CITED

Addadi L, Weiner S. 1985. Interactions between acidic proteins and crystals: stereochemical requirements in biomineralization. Proc Natl Acad Sci 82:4110-4114.

Aizenberg J, Lambert G, Weiner S, Addadi L. 2001. Factors involved in the formation of amorphous and crystalline calcium carbonate: a study of an ascidian skeleton. J Am Chem Soc 124:32-39.

Buchholz F. 1989. Moult cycle and seasonal activities of chitinolytic enzymes in the integument and digestive tract of the Antarctic krill, *Euphausia superba*. Polar Biol 9:311-317.

Byers S, van Rooden JC, Foster BK. 1997. Structural changes in the large proteoglycans, aggrecan, in different zones of the ovine growth plate. Calcif Tissue Int 60:71-78.

Chapman RF. 1982. The Insects: Structure and Function. Cambridge, Massachusetts: Harvard University Press. 919 p.

Coblentz FE, Shafer TH, Roer RD. 1998. Cuticular proteins from the blue crab alter *in vitro* calcium carbonate mineralization. Comp Biochem Physiol 121B:349-360.

Compère P, Goffinet G. 1987a. Ultrastructural shape and three-dimensional organization of the intracuticular canal systems in the mineralized cuticle of the green crab, *Carcinus maenas*. Tissue Cell 19:839-857.

Compère P, Goffinet G. 1987b. Elaboration and ultrastructural changes in the pore canal system of the mineralized cuticle of *Carcinus maenas* during the molting cycle. Tissue Cell 19:859-875.

Compère P, Morgan JA, Goffinet G. 1993. Ultrastructural location of calcium and magnesium during mineralization of the cuticle of the shore crab, as determined by the K-pyroantimonate method and X-ray microanalysis. Cell Tissue Res 274:567-577.

Compère P, Thorez A, Goffinet G. 1998. Fine structural survey of the old cuticle degradation during pre-ecdysis in two European Atlantic crabs. Tissue Cell 30:41-56.

Crenshaw MA. 1982. Biological Mineralization and Demineralization: Mechanisms of Normal Biological Mineralization of Calcium Carbonates. In: Nancollas GH, editor. Dahlem Konferenzen. New York, Heidelberg, Berlin: Springer-Verlag. p 243-257.

Debray H, Decout D, Strecker G, Spik G, Montreuil J. 1981. Specificity of twelve lectins towards oligosaccharides and glycopeptides related to *N*-glycosylproteins. Eur J Biochem 117:41-55.

Dennell R. 1947. The occurrence and significance of phenolic hardening in the newly formed cuticle of Crustacea Decapoda. Proc R Soc Lond B Biol Sci 134:485-503.

Dillaman RM, Hequembourg SJ, Gay DM. 2001. Pattern of extracellular matrix transformation preceding calcification of crab integument. Mol Biol Cell V12 Suppl: p 1889.

Drach P. 1939. Mue et cycle d'intermue chez les crustaces decapodes. Ann Inst Oceanogr 19:103-391.

Elliott EA, Dillaman RM. 1999. Formation of the inner branchiostegal cuticle of the blue crab, *Callinectes sapidus*. J Morphol 240:267-281.

Freeman JA. 1980. Hormonal control of chitinolytic activity in the integument of *Balanus amphitrite*, *in vitro*. Comp Biochem Physiol 65A:13-17.

Giraud-Guille MM, Quintana C. 1982. Secondary ion microanalysis of the crab calcified cuticle: distribution of mineral elements and interactions with cholesteric organic matrix. Biol Cell 44:57-67.

Giraud-Guille MM. 1984a. Calcification initiation sites in the crab cuticle: the interprismatic septa, an ultrastuctural cytochemical study. Cell Tissue Res 236:413-420.

Giraud-Guille MM. 1984b. Fine structure of the chitin-protein system in the crab cuticle. Tissue Cell 16:75-92.

Gomori G. 1950. A new stain for elastic tissue. Am J Clin Pathol 20:665-666.

Green JP, Neff MR. 1972. A survey of the fine structure of the integument of the fiddler crab. Tissue Cell 4:137-171.

Gunthorpe ME, Sikes CS, Wheeler AP. 1990. Promotion and inhibition of calcium carbonate crystallization *in vitro* by matrix protein from blue crab exoskeleton. Biol Bull 179:191-200.

Hackman RH. 1984. Cuticle: Biochemistry. In: Bereiter-Hahn J, Matoltsy AG, Richards KS, editors. Biology of the Integument 1: Invertebrates. Berlin Heidelberg New York Tokyo: Springer-Verlag. p 583-610.

Hadley NF. 1994. Water Relations of Terrestrial Arthropods. San Diego, California: Academic Press. 157 p.

Hegdahl T, Silness J, Gustavsen F. 1977a. The structure and mineralization of the carapace of the crab (*Cancer pagurus* L.): The endocuticle. Zool Scripta 6:89-99.

Hegdahl T, Gustavsen F, Silness J. 1977b. The structure and mineralization of the carapace of the crab (*Cancer pagurus* L.): The exocuticle. Zool Scripta 6:101-105.

Hegdahl T, Gustavsen F, Silness J. 1977c. The structure and mineralization of the carapace of the crab (*Cancer pagurus* L.): The epicuticle. Zool Scripta 6:215-220.

Hequembourg SJ. 2002. Early patterns of calcium and protein deposition in the carapace of the blue crab. M. S. Thesis. University of North Carolina at Wilmington.

Johnson PT. 1980. Histology of the Blue Crab, *Callinectes sapidus*. A Model of the Decapoda. New York: Praegerr Publishers. 440 p.

Kathirithamby J, Luke BM, Neville AC. 1990. The ultrastructure of the preformed ecdysial 'line of weakness' in the puparium cap of *Elenchus tenuicornis* (Kirby) (Insecta: Strepsiptera). Zool J Linnean Soc 98:229-236.

Leiner IE, Sharon H, Goldstein, IJ, editors. 1986. The Lectins. Properties, Functions, and Applications in Biology and Medicine. Orlando, Florida: Academic Press. 600 p.

Levi-Kalisman Y, Raz S, Weiner S, Addadi L, Sagi I. 2000. X-ray absorption spectroscopy studies on the structure of a biogenic "amorphous" calcium carbonate phase. J Chem Soc/ Dalton Trans 2000:3977-3982.

Lowenstam HA, Weiner S. 1989. On Biomineralization. New York, New York: Oxford University Press. 324 p.

Mangum CP. 1985. Molting in the blue crab *Callinectes sapidus*: A collaborative study of intermediary metabolism, respiration and cardiovascular function, and ion transport. Preface. J Crust Biol 5:185-187.

Mangum CP, deFur PL, Fields JHA, Henry RP, Kormanik GA, McMahon BR, Ricci J, Towle DW, Wheatly MG. 1985. Physiology of the blue crab *Callinectes sapidus* Rathbun during a molt. National Symposium on the Soft-Shelled Blue Crab Fishery, February 12-13:1-12.

Marlowe RL, Dillaman RM, Roer RD. 1994. Lectin binding by crustacean cuticle: the cuticle of *Callinectes sapidus* throughout the molt cycle, and the intermolt cuticle of *Procambarus clarkii* and *Ocypode quadrata*. J Crust Biol 14:231-246.

Marlowe RL, Dillaman RM. 1995. Acridine orange staining of decapod crustacean cuticle. Invert Biol 114:79-82.

McKee MD, Zalzal S, Nanci A. 1996. Extracellular matrix in tooth cementum and mantle dentin: localization of osteopontin and other noncollagenous proteins, plasma proteins, and glycoconjugates by electron microscopy. Anat Rec 245:293-312.

Murphy DB. 2001. Fundamentals of Light Microscopy and Electron Imaging. New York: Wiley-Liss. 357 p.

Neville AC. 1975. Zoophysiology and Ecology volume 4/5: Biology of the Arthropod Cuticle. Hoar WS, Jacobs J, Langer H, Lindauer M, editors. New York, Heidelberg, Berlin: Springer-Verlag. 448 p.

O'Brien JJ, Skinner DM. 1987. Characterization of enzymes that degrade crab exoskeleton: I. Two alkaline cysteine proteinase activities. J Exp Zool 243:389-400.

O'Brien JJ, Skinner DM. 1988. Characterization of enzymes that degrade crab exoskeleton: II. Two acid proteinase activities. J Exp Zool 246:124-131.

Passano LM. 1960. Molting and its control. In: Waterman T, editor. The Physiology of Crustacea. Volume I: Metabolism and Growth. New York, San Francisco, London: Academic Press. p 473-536.

Presnell JK, Schreibman MP. 1997. Humason's Animal Tissue Techniques. Baltimore, London: The Johns Hopkins University Press. 572 p.

Rasch R, Cribb BW, Barry J, Palmer CM. 2003. Application of quantitative analytical electron microscopy to the mineral content of insect cuticle. Microsc Microanal 9:152-154.

Raz S, Testeniere O, Hecker A, Weiner S, Luquet G. 2002. Stable amorphous calcium carbonate is the main component of the calcium storage structures of the crustacean *Orchestia cavimana*. Biol Bull 203:269-274.

Reaka ML. 1975. Molting in stomatopod crustaceans. I. Stages of the molt cycle, setagenesis, and morphology. J Morphol 146:55-80.

Roer RD. 1980. Mechanisms of resorption and deposition of calcium in the carapace of the crab *Carcinus meanas*. J Exp Biol 88:205-218.

Roer RD, Dillaman RM. 1984. The structure and calcification of the crustacean cuticle. Am Zool 24:893-909.

Roer R D, Dillaman RM. 1993. Molt-related change in integumental structure and function., In: Horst MN, Freeman JA, editors. The Crustacean Integument: Morphology and Biochemistry. Boca Raton, Florida: CRC Press. p 1-37.

Shafer TH, Roer RD, Midgette-Luther C, Brookins TA. 1995. Postecdysial cuticle alteration in the blue crab, *Callinectes sapidus*: synchronous changes in glycoproteins and mineral nucleation. J Exp Zool 271:171-182.

Simkiss K. 1975. Studies in Biology no53. Bone and Biomineralization. London: Edward Arnold Publishers Limited. 60 p.

Skinner DM. 1962. The structure and metabolism of a crustacean integumentary tissue during a molt cycle. Biol Bull 123:635-647.

Skinner DM. 1985. Molting and regeneration. In: Bliss DE, Mantel LH, editors. The Biology of Crustacea, Vol. 9. Integument, pigments, and hormonal processes. Orlando, Florida: Academic Press, Inc. p 43-146.

Spicer SS, Schulte BA. 1992. Diversity of cell glycoconjugates shown histochemically: a perspective. J Histochem Cytochem 40:1-38.

Spindler KD, Buchholz F. 1988. Partial characterization of chitin degrading enzymes from two euphausiids, *Euphausia superba* and *Meganyctiphanes norvegica*. Polar Biol 9:115-122.

Spindler KD, Funke B. 1989. Characterization of chitinase from the brine shrimp *Artemia*. Comp Biochem Physiol 94B:691-695.

Spindler-Barth M, Van Wormhoudt A, and Spindler KD. 1990. Chitinolytic enzymes in the integument and midgut-gland of the shrimp *Palaemon serratus* during the moulting cycle. Mar Biol 106:49-52.

Spurr AR. 1969. A low viscosity epoxy resin embedding medium for electron microscopy. J Ultrastruct Res 26:31-43.

Stevenson JR. 1968. Metecdysial molt staging and changes in the cuticle in the crayfish *Orconectes sanborni* (Faxon). Crustaceana 14:169-177.

Stevenson JR. 1972. Changing activities of the crustacean epidermis during the molt cycle. Am Zool 12:373-380.

Stumm W, Morgan JJ. 1981. Aquatic Chemistry: an Introduction Emphasizing Chemical Equilibria in Natural Waters. New York: Wiley-Interscience. 780 p.

Summers NM Jr. 1967. Cuticle sclerotization and blood phenol oxidase in the fiddler crab, *Uca pugnax*. Comp Biochem Physiol 23:129-138.

Summers NM Jr. 1968. The conversion of tyrosine to catecholamines and the biogenesis of N-acetyl-dopamine in isolated epidermis of the fiddler crab, *Uca pugilator*. Comp Biochem Physiol 26:259-269.

Thompson SW. 1966. Selected Histochemical and Histopathological Methods. Springfield, Illinois: Charles C. Thomas Publisher. 1639 p.

Travis DF. 1955a. The molting cycle of the spiny lobster, *Panulirus argus* Latreille. II Pre-ecdysial histological and histochemical changes in the hepatopancreas and integumental tissues. Biol Bull 108:88-112.

Travis DF. 1955b. The molting cycle of the spiny lobster, *Panulirus argus* Latreille. III. Physiological changes which occur in the blood and urine during the normal molting cycle. Biol Bull 109:484-503.

Travis DF. 1957. The molting cycle of the spiny lobster, *Panulirus argus* Latreille. IV Post-ecdysial histological and histochemical changes in the hepatopancreas and integumental tissues. Biol Bull 113:451-479.

Travis DF. 1963. Structural features of mineralization from tissue to macromolecular levels of organization in the decapod Crustacea. Ann N Y Acad Sci 109:177-245.

Travis DF. 1965. The deposition of skeletal structures in the Crustacea. 5. The histomorphological and histochemical changes associated with the development

and calcification of the branchial exoskeleton in the crayfish, *Orconectes virilis* Hagen. Acta Histochem 20S:193-222.

Travis DF, Friberg U. 1963. The deposition of skeletal structures in the Crustacea. VI. Microradiographic studies of the exoskeleton of the crayfish *Orconectes virilis* Hagen. J Ultrastruct Res 9:285-301.

Vacca LL, Fingerman M. 1975. The mechanisms of tanning in the fiddler crab, *Uca pugilator*. I. Tanning agents and protein carriers in the blood during ecdysis. Comp Biochem Physiol 51B:475-481.

Vinogradov AP. 1953. The Elementary Chemical Composition of Marine Organisms. Sears Foundation for Marine Research, New Haven, Connecticut: Yale University. 647 p.

Vogel S. 1988. Life's Devices: The Physical World of Animals and Plants. Princeton, New Jersey: Princeton University Press. 367 p.

Wheeler AP, Rusenko KW, Swift DM, Sikes CS. 1988. Regulation of *in vitro* and *in vivo* $CaCO_3$ crystallization by fractions of oyster shell organic matrix. Mar Biol 98:71-80.

Williams CL, Dillaman RM, Elliott EA, Gay DM. 2003. Formation of the arthrodial membrane in the blue crab, *Callinectes sapidus*. J Morphol 256:260-269.

Young NM, Watson DC, Thibault P. 1996. Post-translational proteolytic processing and the isolectins of lentil and other Viciae seed lectins. Glycoconj J 13:575-583.

Zar JH. 1999. Biostatistical Analysis 4th ed. Upper Saddle River, New Jersey: Prentice-Hall. 663 p.

BIOGRAPHICAL SKETCH

Carolina Priester was born in Sao Paulo, Brazil, on March 12th, 1975. She obtained her Bachelor of Arts in Communication Studies in December of 1997 from the 'Escola Superior de Propaganda e Marketing' at Sao Paulo, Brazil. She then transferred to the University of North Carolina at Wilmington where she completed her Bachelor of Science degree in Marine Biology with a minor in Chemistry in 2001. She enrolled in the graduate program at the University of North Carolina at Wilmington where she will receive a Master of Science degree in Biology in 2003. During her graduate experience she worked as a teaching assistant and research assistant in the UNCW Biological Sciences department. In her spare time she worked as a building manager coordinator for the UNCW University Union and as a graduate hall director for the UNCW Housing and Residence Life. She is currently a member of Sigma Xi and the Society for Marine Mammalogy. She has participated with poster presentations at the 14th Biennial Conference on the Biology of Marine Mammals, Vancouver, Canada, 2001, and at the Microscopy and Microanalysis 2003 Conference in San Antonio, TX, August 3rd-7th, where she was awarded first place in the Biological Sciences Category and her poster was chosen for the Microscopy Society of America's Traveling Poster Exhibit. She has also participated with an oral presentation at The Crustacean Society meeting in Williamsburg, VA, June 1st-6th, 2003. She would like to continue researching in the biological sciences field, pursue her Ph.D. and teach at the university level.